AD-A077 869 WESTINGHOUSE DEFENSE AND ELECTRONIC SYSTEMS CENTER B--ETC F/G 17/5
INTELLIGENT TRACKING TECHNIQUES.(U)
APR 79 T J WILLETT

UNCLASSIFIED DAAK70-78-C-0167
NL

1 OF 2
AD A077869

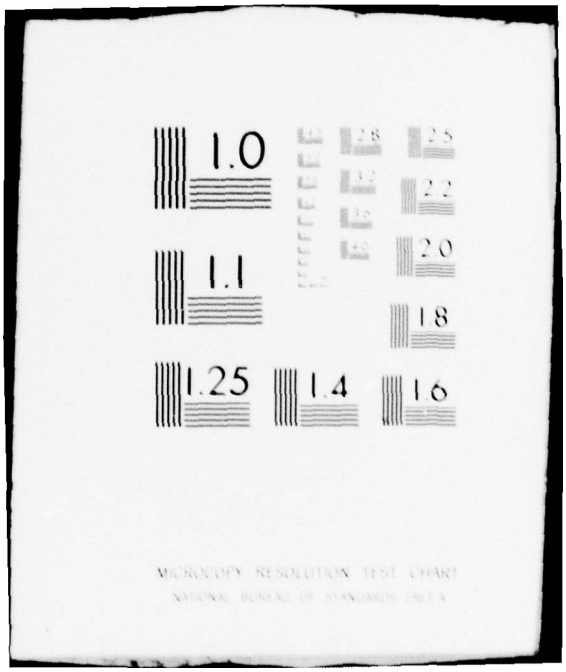
1.0
1.1
1.25
1.4
1.6
2.0
1.8
2.2
2.5
MICROCOPY RESOLUTION TEST CHART

LEVEL III

INTELLIGENT TRACKING TECHNIQUES

SECOND QUARTERLY REPORT

for

March 30, 1979

CONTRACT DAAK 70-78-C-0167

Presented to

UNITED STATES ARMY
Night Vision and Electro-Optics Laboratory
Fort Belvoir, Virginia 22060

Submitted by

Westinghouse Electric Corporation
Systems Development Division
Baltimore, Maryland 21203

SECURITY CLASSIFICATION OF THIS PAGE (When Data Entered)

REPORT DOCUMENTATION PAGE

READ INSTRUCTIONS BEFORE COMPLETING FORM

1. REPORT NUMBER

2. GOVT ACCESSION NO.

3. RECIPIENT'S CATALOG NUMBER

4. TITLE (and Subtitle)
Intelligent Tracking Techniques.
Second Quarterly Report

AD71666

5. TYPE OF REPORT & PERIOD COVERED
Second Quarterly Report
Jan. 1 - March 30, 1979

6. PERFORMING ORG. REPORT NUMBER

7. AUTHOR(s)
T.J. Willett [redacted]
Thomas

8. CONTRACT OR GRANT NUMBER(s)
DAAK-70-78-C-0167

9. PERFORMING ORGANIZATION NAME AND ADDRESS
Systems Development Division
Westinghouse Electric Corporation
Baltimore, MD 21203

10. PROGRAM ELEMENT, PROJECT, TASK AREA & WORK UNIT NUMBERS

11. CONTROLLING OFFICE NAME AND ADDRESS
U.S. Army
Night Vision & Electro-Optical Laboratory
Fort Belvoir, VA 22060

12. REPORT DATE
April 30, 1979

13. NUMBER OF PAGES
95

14. MONITORING AGENCY NAME & ADDRESS (if different from Controlling Office)
Quarterly rept. no. 2.
1 Jan - 30 Mar 79,

15. SECURITY CLASS. (of this report)
Unclassified

15a. DECLASSIFICATION/DOWNGRADING SCHEDULE

16. DISTRIBUTION STATEMENT (of this Report)
Distribution Unlimited

DISTRIBUTION STATEMENT A
Approved for public release;
Distribution Unlimited

17. DISTRIBUTION STATEMENT (of the abstract entered in Block 20, if different from Report)

18. SUPPLEMENTARY NOTES

19. KEY WORDS (Continue on reverse side if necessary and identify by block number)
Automatic Target Cueing
Target Recognition
Target Tracking
FLIR Sensor
Digital Image Processing
Correlation Tracker

20. ABSTRACT (Continue on reverse side if necessary and identify by block number)
This is the Second Quarterly Report under a contract to investigate the design, test, and implementation of a set of algorithms to perform intelligent tracking and intelligent target homing on FLIR and TV Imagery. The intelligent tracker will monitor the entire field of view, detect and classify targets, perform multiple target tracking and predict changes in target signature prior to the target's entry into an obscuration. The intelligent tracking and homing system will also perform target prioritization and critical aimpoint selection.

DD FORM 1 JAN 73 1473 EDITION OF 1 NOV 65 IS OBSOLETE

UNCLASSIFIED 405 897

SECURITY CLASSIFICATION OF THIS PAGE (When Data Entered)

The intelligent tracker was defined in terms of its functions and a systems analysis of those functions led to a set of constraints. Analysis of the intelligent tracker embedded in AAH, RPV, and PGM scenarios provided additional system requirements and goals. The base line frame to frame tracker was described and a number of variations. An effort was devoted to restructure the segmentation algorithms to sharpen their ability to segment small targets (4 lines high) in heavy clutter. Target signature prediction was analyzed in terms of two examples from the NV&EOL data base. Also included is a description of the NV&EOL TV data base.

INTELLIGENT TRACKING TECHNIQUES

SECOND QUARTERLY REPORT

for

March 30, 1979

CONTRACT DAAK 70-78-C-0167

Presented to

UNITED STATES ARMY

Night Vision and Electro-Optics Laboratory

Fort Belvoir, Virginia 22060

Submitted by

Westinghouse Electric Corporation
Systems Development Division
Baltimore, Maryland 21203

Table of Contents

Table of Contents (Con't)

INTRODUCTION

Under contract to the Army's Night Vision and Electro-Optics Laboratory, Westinghouse has been investigating the design, test, and implementation of a set of algorithms to perform intelligent tracking and intelligent target homing on FLIR and TV imagery. Research has been initiated for the development of an intelligent target tracking and homing system which will combine target cueing, target signature prediction, and target tracking techniques for near zero break lock performance. The intelligent tracker will monitor the entire field of view, detect and classify targets, perform multiple target tracking and predict changes in target signature prior to the target's entry into an obscuration. The intelligent tracking and homing system will also perform target prioritization and critical aimpoint selection. Through the use of VLSI/VHSI techniques, the intelligent tracker (with inherent target cuer) can be applied to the fully autonomous munition.

During the second quarter, several meetings and a number of phone conversations took place between Westinghouse personnel and John Dehne, Peter Raimondi, and Capt. Ben Reischer of NV & EOL. The intelligent tracker was defined in terms of its functions and a systems analysis of those functions led to a set of constraints. Analysis of the intelligent tracker embedded in AAH, RPV, and PGM scenarios provided additional system requirements and goals. The base line frame to frame tracker was described and a number of variations examined. The strategy is to start with a simple tracker and work toward more sophisticated designs as required to handle the NV & EOL data base scenarios. An effort was devoted to restructure the Smart Sensor pre-processing algorithms to sharpen their ability to segment small targets

(4 lines high) in heavy clutter. This situation is an outgrowth of the RPV scenario analysis. Target signature prediction was analyzed in terms of two examples from the NV & EOL data base. Also included is a description of the NV & EOL TV data base.

Westinghouse personnel participating in this effort include Thomas Willett, Program Manager; Dr. John Romanski, John Shipley, Leo Kossa, Tony Canigiliosa, Robert Bidney and Richard Kroupa. Program Review and consultation is provided by Drs. Glenn Tisdale and Azriel Rosenfeld.

1.0 Systems Considerations

The purpose of this section is to define the intelligent tracker in terms of its functions, to describe the range of possible system concepts, to define three scenarios in which the intelligent tracker will play a part, to describe the range of technical problems in developing each of the functions, and to derive system requirements and goals from an analysis of the scenarios.

1.1 Intelligent Tracker - A Functional Definition

In the first quarterly report, the concept of the "intelligent tracker" was explained in terms of desired performance improvement over conventional trackers. In a detailed design analysis, however, it may be more useful to define it in terms of its functions. The functions are:

1) acquisition and handoff to tracker- locate, detect, classify, and prioritize targets automatically and hand off to a tracker (The "intelligent tracker" concept is assumed to include both acquisition and tracking);
2) handle multiple targets- track a number of targets in a scene simultaneously;
3) target signature prediction- predict or anticipate target occlusions and how the target signature will change as a result of the obscuration;
4) reacquisition- reacquire a target as a result of track break lock or if it leaves the field of view;
5) aimpoint selection- determine the critical aimpoint of a target, which may be an interior point within its outline.

1.2 Possible System Concepts

The system concepts which are available to implement the above functions range from a highly sophisticated tracker to a high-speed cuer. Between these extremes is a cuer-tracker combination. The tradeoffs associated with each concept will be examined under this contract. The highly sophisticated tracker is assumed to operate at frame or field rates, but to lack the capability for automatic acquisition and multiple target track. At the other end of the spectrum, the stand alone cuer will have automatic acquisition capability, but it might not possess adequate tracking speed or the ability to handle high frame rates. The combination of distinct cuer and tracker logic in an integrated "intelligent tracker" system may offer desired performance with a minimum of hardware complexity and required speed. However, the design problems may be more complex.

1.3 Application in AAH, RPV, or PGM Scenarios

Three application areas will be considered later in this section to provide intelligent tracker system goals or requirements. These are the AAH, RPV, and PGM vehicles. The AAH scenario consists of a helicopter in a pop-up mode firing a group of missiles at a cluster of targets whose position is known well enough to get the helicopter within viewing range but not well enough to provide a fire control solution. The RPV scenario consists of an RPV acquiring a target at detection range, closing on the target to classification range, and then returning to detection range to track it. The PGM scenario includes a smart artillery shell which is fired at a target from a ground range on the order of 10 km or greater.

1.4 Analysis of Intelligent Tracker Functions

The functions described in Para. 1.1 will now be discussed in terms of the technical problems associated with their development and in terms of the system goals and requirements which can be obtained by considering the three above scenarios. A cuer-tracker combination is assumed.

1.4.1 Acquisition and Handoff

This function includes four sub-functions: detection, classification, target prioritization, and target hand-off to the self-contained tracker. These will be discussed in order.

1.4.1.1 Detection Rate

Determination of the required detection rate will involve an analysis of the overall system in which the intelligent tracker is embedded. For purposes of illustration, however, let us assume a minimum bound on the probability of detection of ≥ 0.995. A survey by NV&EOL indicates that the present single frame detection performance is of the order of 0.90. By combining the results of several frames, however, this single frame performance can be improved. This improvement will now be considered.

If we assume target detections are independent from frame to frame, then the probability of detection on x frames out of n frames follows the cumulative binomial distribution.

$$P(x) = \sum_{x=1}^{n} \binom{n}{x} p^{x}(1-p)^{n-x},$$

where p is the probability of detection on a single frame. Figure 1.0-1 shows the cumulative detection probability against the number of detections for a given number of looks, with a single look probability of detection

of 0.90. We are using multiple looks to drive the overall probability of detection to $\geq$ 0.995. Figure 1.0-1 shows that at least four looks at the target are required to exceed a overall detection probability of 0.995.

Number of Looks (Frames)	Min. Number of Detection	Cumm. Prob. of Detection
2		
3		
4	3	.995
5	4	.998
6	4	.999
7	4	.997
8	4	.995
9	5	.999
10	6	.998

Figure 1.0-1. Cumulative Prob. of Detection vs. Number of Detections (P_D = 0.90 for Single Look)

1.4.1.2 Classification

With regard to classification, we make several simplifying assumptions, namely that the classifications are independent frame to frame and the probability of a correct classification is .65. This latter assumption means that the probability of classifying an APC as an APC is .65; the probability of classifying the APC as anything (e.g. jeep) else is .35 on a single frame. The problem with putting the classification problem in these terms is that no particular classification may dominate after (e.g. 6 frames) and hence other decision procedures are required. This approach does point out that a large number of frames is required and the probability of classification of .65 should be raised to $\geq$ .85 or so before multiple looks (classifications) are useful. Figure 1.0-2 shows the cumulative binomial probability distribution for a single frame probability of classification of 0.65. Figure 1.0-2 indicates that the minimum number of looks at the target under the assumptions described above is six.

The reason that the assumed system probabilities of detection and classification are selected so high is that the overall probability of effectiveness of the system in which the intelligent tracker is embedded will be a product of many probabilities; e.g. probability of impact, probability of kill, etc. Multiplication of a number of probabilities ensures that the final product will be less than the lowest component.

Number of Looks	Min. No. of Correct Classifications	Cum. Prob. of Classification
2	-	< .995
3	-	< .995
4	-	< .995
5	-	< .995
6	6	.995
7	7	.998
8	7	.996
9	8	.998
10	8	.995

Figure 1.0-2. Cumulative Probability of Classification vs. Number of Classification (Probability of Correct Classification on a Single Look in 0.65)

1.4.1.3 Target Prioritization

Target prioritization follows the classification (tank, truck, APC, etc.) by directing attention to that target considered most important. The order of importance is probably determined prior to the mission. The intelligent tracker will classify targets and order them in accordance with an a priori hierarchy. List processing is required to reorder the classified targets

according to some priority. The coordinates and reference image of the highest priority target are made available to the tracker.

1.4.1.4 Handoff to the Internal Tracker

The technical problem here is a result of target motion between the time the cuer finishes a frame and the tracker is given the target position. How do we position the tracker on a target whose position is no longer known and to what degree is it unknown? To address these questions, we will invoke several assumptions. Assume the target (3 meters by 3 meters in size) is traveling at 40 miles per hour (approximately 20 meters per second). Assume also a sensor resolution of 0.33 meters per pixel, and a frame rate of 30 frames per second. Then a vehicle traveling 40 miles an hour and perpendicular to the line of sight (cross-track) moves 2 pixels per frame. Figure 1.0-3 shows the track window size necessary to encompass the target at various cuer frame rates, assuming the direction of motion of the target is unknown and equally likely in all directions.

Frames/Sec.	Distance Moved Plus 1/2 Target Length	Track Window
2	29	58 x 58
3	25	50 x 50
4	21	42 x 42
5	17	34 x 34
6	15	30 x 30
7	13.6	27 x 27
8	12.5	25 x 25
9	11.66	24 x 24
10	11	22 x 22
15	9	18 x 18
30	7	14 x 14

Figure 1.0-3. Frame Rate vs. Track Window Size

All of the track window sizes shown by Figure 1.0-3 are outside the range of desirability. As we have seen in the simulation runs on the NV&EOL data base, the initial track window should be as small as possible from the standpoint of locking up on a false alarm, or on another target within close proximity to the first one. Special algorithms are used for an initial track window of 32 x 32 pixels which takes added time and impinges on the multiple target tracking problem discussed later in this section. Hence, for accurate handoff to an internal tracker, the cuer frame rates should be as fast as possible. For example, for a 9 x 9 pixel target, a desirable track window would be 12 x 12 pixels, which requires a frame rate upwards of 15 frames per second. This analysis assumes that the first target cued in the frame is not handed to the tracker until the last target cued in the frame has been processed. To partially relieve the pressure for high frame rates, let us hand off to the tracker as soon as a target is cued within the frame, even though the frame processing has not been completed.

In actuality, some cuers use pipeline architecture such that a target in the top portion of the image is segmented and classified as soon as its pixels are available. To illustrate this point, Figure 1.0-4 shows the time occurrence of video at 30 frames per second and the cued frames at the rate of 6 frames per second. The heavy vertical lines represent the cued frames and the smaller, thinner lines represent the tracked frames. The numbers above the horizontal line represent the five frames in a cycle which is repeated beginning at the sixth frame. Normally, the cuer results are available to the tracker somewhere between the fifth and sixth frame; the cuer results are denoted by the arrow labelled CR. Also shown at the bottom of Figure 1.0-4 is the image being processed. If we divide the images into, say, five horizontal

strips, the cuer results of processing strip 1 are available to the tracker around the time of track frame no. 2. In this case the tracker picks up the target from the cuer on the very next frame resulting in an effective 30 frames per second cueing rate and a 14 pixel by 14 pixel track window.

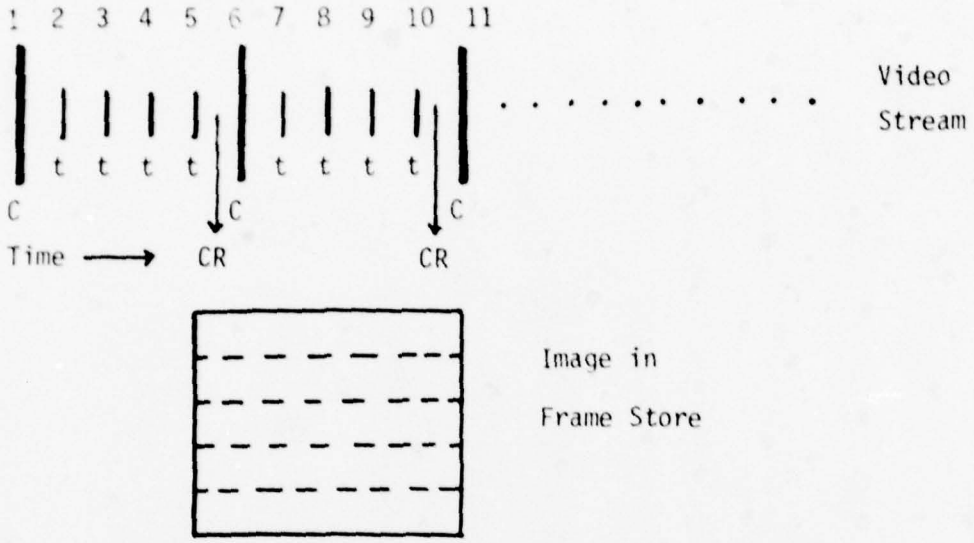

Figure 1.0-4. Cued Frames and Image

The results of strip 2 are available at track frame no. 3 simulating a 15 frames per second cueing rate and a 18 x 18 pixel track window. These window sizes are within the realm of straight-forward tracking hardware. A five frame delay occurs at strip 5. However, on the next cued frame, strip 5 could be read first thus allowing a lag of only one frame.

Thus, even though the scene is scanned by the sensor in only one direction, the scene is placed in a frame storage device which is organized in 5 horizontal sectors, each of which is separately addressable. To avoid problems of cutting targets in half, i.e. when the target falls on a line between two sectors, a five line overlap between sector boundaries is suggested.

To summarize, by the use of appropriate addressing mechanism in the frame storage device, initial track windows approaching the desired 16x16 pixel size, can be used.

1.4.2 Multiple targets

Current trackers generally handle only one target within a given frame; handling multiple targets involves duplicate hardware. This may not be an appropriate solution to the problem at hand because of hardware volume constraints. However, the combination of a cuer with a tracker means that some of the pre-processing normally done by the tracker has already been accomplished. Further, the reference image, assuming a short handoff time, is accurately positioned and described within the image. The synergism then between the cuer and tracker in terms of shared functions leads one in the direction of simpler, faster trackers which can handle a number of targets simultaneously. An example of a simpler, faster tracker is the binary correlation tracker. Lab experiments were conducted at Westinghouse with an existing binary correlation tracker and the F-16 bit-sliced microprocessor used to implement the fire control radar. The bit-sliced microprocessor instruction set was used to compute the best match position and compute the track position error for the binary tracker. A position error for a 16 x 16 track window was computed in approximately 1 millisecond. Against a frame rate of 30 frames per second or 33 milliseconds between frames this implies that a single tracker could handle 30 targets per frame. If we assume that interface delays between a reduced version of the F-16 bit-sliced microprocessor and the binary tracker reduce this number by one half, then a more conservative estimate is 15 targets per frame per tracker. If we restrict our attention to the binary correlation and reference image storage portions of the tracker and ignore the gimbal control, signal conditioning, and so on, the present hardware package is on the order of a 5 x 8 inch board, assuming the tracker is

built in conventional, wire wrapped boards with standard dual in line packs. Additional volume in required for the 14 rams which will hold reference images for the added targets. On the other hand, substantial reductions in hardware volume are anticipated under the Very High Speed Integrated Circuits (VHSIC) Program. A discussion of the binary correlation tracker and several versions of it are contained in a later section of this report.

1.4.3 Target Signature Prediction

This function involves predicting or anticipating target occlusions and predicting how the target signature will change as a result of the obscuration. The most immediate issue that comes to mind is the extent of the prediction process. For example, is it necessary to identify the context within which the target is found in order to perform target prediction? More specifically, is it necessary to identify trees, woods, roads and so on? The answer is not clear; however, it is clear that although much work has been done in identifying context and texture, progress is limited. Further, in view of the scope of the intelligent tracker work, this area of investigation is necessarily limited.

There are a number of obscuration cases which can be predicted with histogram techniques. A histogram of the background in front of the target is examined for gray level content similar to that of the target. Noting such a similarity alerts the intelligent tracker to an impending obscuration. Analysis of the histogram will affect tracker strategy, change detection thresholds, and direct segmentation slices. It may also be possible, using histograms, to detect the disappearance of a target and thereby aid the cuer. Further, the synergism between cuer and tracker comes into play because much of this work can be based on histograms which are used jointly by both the

cuer and tracker. Consider the use of a bandpass binary correlation tracker where the gray levels used in the correlation must fall within a certain band. The histogram over the cued target can be used to update the tracker bandpass every few frames and avoid the common problem whereby due to a change in lighting, background and so on, the target passes out of the bandpass. In Section 2.0 of this report we will discuss the problem of insuring adequate shape description over that part of the target not obscured so that the tracker will have a well-defined reference image composed of that part of the target which is not obscured. This is particularly applicable to small targets which appear in the RPV scenario to be discussed in Section 1.5.

1.4.4 Reacquisition

Reacquisition involves reacquiring a target after a track break lock or a target leaving the field of view. In the former case, the reacquisition is probably the most difficult problem for the intelligent tracker. Consider the case where a target completely disappears from view because it enters a heavy woods. To complicate matters further assume the target is light against a dark background and some of the clearings in the woods also appear light-colored. Further, the target re-emerges and remains partially obscured; this means that the classification logic does not have the benefit of a look at the total target. Finally, the sensor platform has shifted position in the meantime so that the shadows and gray levels appear differently from that image in which the target disappeared. Because the target may be moving in different background than when it disappeared, it may appear as a light target against a lighter background or a dark target against a light background. The solution may lie in examining the histogram content of the various segmented objects or blobs. We are currently working on this scenario and will report on it in the next report.

The other reacquisition problem may involve the same cuer considerations as described above but the target has disappeared because it moved out of the field of view. The track algorithms update the track window position so a history of updates provide the general direction and velocity of the target with respect to the image coordinates. Since the sensor is moved to center the track window in the image according to the tracker window update coordinates, the sensor can also be moved in a like manner to accommodate a Δx, Δy track change based on a predicted target position with respect to the image based coordinate system since the target disappeared from view. The problem is to produce a smoothed track from a series of track window updates because in the multiple target tracking section we discussed the feasibility of providing simulataneous tracking on multiple targets. Without that capability the track prediction problem is much more difficult. This problem also means that a smoothed track must be maintained on all targets of interest being tracked because any one of them could leave the field of view unexpectedly.

Finally, since the sensor control loop is a rate loop and not a position loop, the Δx, Δy pixel position must be mapped into 2nd order difference equations to command the loop to move to a new position and stop. If the command is too strong, the system will overshoot.

1.4.5 Aimpoint Selection

This function has to do with determining the critical aimpoint of a target which at closer range will be a particular interior point on the target silhouette. Critical aimpoint at long range is based on a knowledge of the target classification an the exterior shape. As the range closes, as in a homing situation, more of the interior detail becomes available and the critical aimpoint could now be based on this. The aimpoint algorithm must be compatible with the frame to frame tracker. In this regard, it is envisioned that once the portion of the target which contains the critical aimpoint is identified.

this will become the reference image for the frame to frame tracker. Then, based on the details of this area the critical aimpoint will be selected. This is an update of the aimpoint algorithm at long range. The cuer must identify the aimpoint area.

1.5 Application Areas

The three scenarios to be analyzed for further system requirement and goals involve the (AAH) Advanced Attack Helicopter, the RPV, and the PGM in the form of a smart artillery round.

1.5.1 AAH Scenario

Assume, for this scenario, that the helicopter has located the targets but not to the degree of accuracy which would provide a fire control solution. The helicopter pops up above the trees, analyzes the scene, and fires a number of missiles at the detected and classified targets. Let us make several more assumptions, which may oversimplify the problem, but will nevertheless provide some idea of the order of magnitude of the numbers involved. Suppose the time to detect, classify, and track the targets is measured from the time the sensor is looking at the targets. That is, during the pop up and for a short time thereafter the operator is trying to train the sensors on the targets. During the time the helicopter is visible to the hostile forces, they are taking defensive action against the helicopter. Let us suppose that the helicopter has something on the order of 20-30 seconds to detect, classify, track and fire. Further, we assume that the missile sensors are slaved to the helicopter sensor. Also, the missile payload is 10 missiles and there are 15 targets within the sensor field of view. We want the number of targets to exceed the missile payload so that target prioritization is exercised. Assume, further, that the pop up range and sensor resolution are such that the helicopter is within classification range of the targets. If the missiles are fired sequentially over the period of say 25 seconds, and the platform reaction to each

firing is such that the sensor must be realigned on the targets (a case for reacquiaition when the target leaves the field of view), then the time remaining for detection, classification, and track is reduced. Assume that reaction and realignment is of the order of one second, this leaves approximately one second for detection, classification, target prioritization and target establishment per target and per missile launch. Detection, classification, and track establishment is conducted on targets approximately 9 lines high. If we refer to the previous discussion on track window sizes, we see that the maximum number of pixels any target can travel (maximum cross track velocity of 20 meter/sec.) is 600 pixels. That is during the 25 seconds, a high speed target could travel across the entire field of view. The maximum amount a particular target could travel from detection to a missile launch on it is 60 pixels. Further for a high system probability of correct classification (0.995), 6 looks at the target are required so the frame rate must be at least 6 frames per second. There are additional ramifications to the AAH scenario.

Fifteen multiple target tracks must be maintained on the detected targets without regard to the ultimate classification of each. That is, under the above scenario suppose six cued frames are required for classification. Fifteen targets are detected on the first to 5th cued frames and multiple tracks are established. The frame store device is addressable in the manner described previously, i.e. 5 horizontal strips, and the addressing rotated such that there is a minimum lag between a cued frame and a track frame. The highest priority target is selected on the 6th frame and the missile is launched. On the 6th frame, the 2nd highest priority target is also selected and will serve to guide the sensor reacquisition following the missile launch reaction, if any. This discussion leads to the following possible variation in the system concept.

1.5.1.1 System Concept Variation-Frame Rate Cueing of Detected Targets

Previously, we discussed the range of possible intelligent tracker system concepts from a very sophisticated tracker to a stand alone cuer. If we wish to increase the frame rates, as it now appears necessary, to enhance classifications, reduce track window sizes, and reduce the lag between cued frames and tracked frames, there appears to be a possible solution in favor of a stand alone cuer. Referring to Figure 1.0-4, we see that a 16 x 16 track window is adequate to encompass the target 9 x 9 pixels at maximum velocity on the next frame. If we assume that 15 targets are present, then a total of 15x16x16 = 3840 pixels are snatched from the video stream. Recall that the track windows are snatched from the video stream at frame rates. If these pixels were processed by the cuer at frame rates, the equivalent pixel rate is 115,000 pixels/sec.; this is $115\times10^{3} / 6\times330\times10^{3} = 1/24$ of the processing rate at 6 frames per second. This raises the possibility that a separate, lower speed cuer implemented in a smaller volume, slower solid state technology could be used to classify and track designated targets for the frames not covered by the 6 frame per second cuer. This configuration then would consist of a 6 frame or greater per second acquisition cuer, with a smaller, slower frame by frame cuer which would classify acquired targets within a 16 x 16 window. This concept raises the number of cued looks per target and should increase classification performance accordingly. Of course, the issue here is the particular form of hardware implementation which does not increase the hardware volume significantly.

1.5.2 RPV Scenario

The RPV, in some cases, will make a detection on a target at maximum detection range, move in to perform classification, and then move back to detection range and track the target. At maximum detection range the target is four lines high and at maximum classification range the target is eight to ten lines high. In this case the previously described concept of multiple target

tracking is appropriate because multiple target tracks are continued on the detected targets as the RPV closes for classification. These tracks will serve to control the sensor position such that the maximum number of targets remain in the image during the transition to a shorter range. The process of detection, closing, classification, and establishing a stand-off position is probably accomplished in a longer time period than that required by the AAH scenario. However, in the RPV case there is a premium on maintaining track on small targets, i.e. four lines high from a stand-off position when the track must be held longer than in either the AAH or PGM Scenarios. In Section 2.0, we shall address the issue of sharpening the preprocessing functions in anticipation of this problem.

1.5.3 Smart Artillery Shell

For the PGM, Precision Guided Munition, which probably takes its ultimate form in the smart artillery shell the scenario is more difficult to analyze. Let us make several simplifying assumptions. Assume that the highest priority target must be selected at a range of 1500 meters from impact. Assume, further, that the vehicle is closing at 500 meters/sec. and is not spinning. The ground range is assumed to be 20,000 meters and the unguided CEP is that of a 155 mm shell, namely 300 meters. At 1500 meters, the 300 meter CEP, 600 meter diameter circle, ground coverage is of the order of 23^{o}; at 3000 meters, the ground coverage is 12^{o}. The required resolution for classification is ½ meter per pixel, so the image is 1200 pixels high. The image to be processed is of the order of 1.44 mega pixels which is roughly four times as large as the conventional 500 x 650 TV image. We assume that the range at which the ½ meter per pixel resolution occurs is somewhere between 3000 and 2000 meters. This is equivalent to three seconds maximum and one second minimum to reach a classification decision at a closing speed of 500 meters per second.

If we assume a 3g missile, the maximum diversion from 3000 meters to 1500 meters is ± 132 meters. Further, from 1500 meters to impact, the additional maximum lateral movement is another ±132 meters. Hence, for a 3g missile, the maximum spot on the ground as constrained by projectile kinematics is approximately 300 meters or equivalent to a 150 meter CEP. At a resolution of ½ meter/pixel, the image is 600 pixels high. That is, it is approximately the same size as the TV image. At cueing rate of 6 frames per sec., the required data rates are equivalent to those of the RPV and AAH scenarios, namely two megapixels/sec.

The conflict between the CEP allowed by missile kinematics and that provided by the artillery piece is being analyzed under the Advanced Pattern Matching work sponsored by NV&EOL. Here, the projectile performs pattern matching on the target surroundings and steers even before the target is detected. Note that the reference image is provided by an RPV and the reference image is no older than five (5) minutes. This approach affects the scenario we described, because we assumed steering on the target at 3000 meters. This may not be necessary in the semi-autonomous case and may also result in a lower required data rate. The point here is that it is not axiomatic that the smart artillery shell requires high image processing rates.

1.6 Summary

In order to obtain high levels of system performance for detection and classification, under the stochastically independent assumption for each process, it appears that multiple looks at the target are required. To achieve multiple target tracking capability at high rates and reasonable target volume, fairly simple trackers will probably be necessary. The cuer then plays a prominent role in providing reference windows and updating capability to the tracker. The AAH scenario suggests that detection, classification, prioritization and track

establishment be accomplished in one second. The RPV scenario places a premium on tracking small targets in obscuration and the PGM scenario does not call for an excessive data handling capability. To ensure a small track window, the time lag between cuer and track should be minimized by sequencing the frame storage device. Multiple smoothed tracks must be maintained on all targets to ensure that the sensor can swing back to a high priority target which has left the field of view. Finally the idea of adding a small, lower speed cuer in a different solid state technology to handle targets cued by the acquisition (6 frames/sec.) cuer would enhance both tracking and classification capability. The additional cuer would operate at a lower data rate but provide a faster update on a smaller image area. The lower data rate and small volume may mean employing a different solid state technology.

2.0 ALGORITHM MODIFICATIONS TO ACCOMMODATE OBSCURATIONS

The purpose of this section is to describe algorithm improvements necessary to track small targets (for example, four lines high) through obscurations. A stand-off RPV scenario is assumed. The problem of tracking through obscurations is described, the preprocessing algorithms are reviewed, a variation of the algorithms to enhance edges is described, and the variation is compared with the standard preprocessing algorithms for edge content. We described several kinds of obscurations in Section 1.4.3 (Target Signature Prediction) in which the gray scale levels of the target are the same as the background which the target is entering. We can imagine scenarios where the target is encountering obsucrations in the vertical or horizontal directions. That is, if there are low lying shrubs as seen in Figure 2-1, we want as much definition on the upper part of the target as possible. In terms of the algorithms described in Appendix

Figure 2.0-1. Horizontal Obscuration

A of the First Quarterly Report, we want a number of significant edges to remain after thinning, and we want good coincidence of these edges and target's perimeter points determined from slicing. We shall review these algorithms in the next section (Par. 2.1). If the obscuration were vertical as in Figure 2.0-2, the same requirements apply, except to the rear of the target. Similar kinds of remarks apply to the case where the tree is darker than the target or the same gray level as the target. The object does not have to be a tree, for the reader can imagine the obscuration as a road or even another target. A first approach to tracking through this kind of obscuration is now described.

Figure 2.0-2 Vertical Obscuration

We assume the obscuration is sensed ahead of time and the target signature prediction algorithms realize in the case of Figure 2.0-2 that the front of the target will soon be lost. The question now is, what constitutes the reference image for the tracker? We give up the front part of the target and instead of centering the entire target in the window, we center the rear portion as shown in Figure 2.0-3. At the same time, we begin looking for

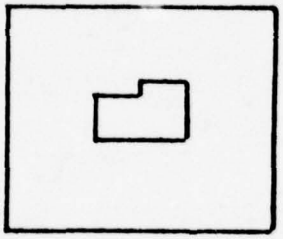

Figure 2.0-3 Track Window For
Disappearing Target

the emerging front edge either through direct segmentation or change detection. Having detected the emerging front portion, the new track window is shown in Figure 2.0-4.

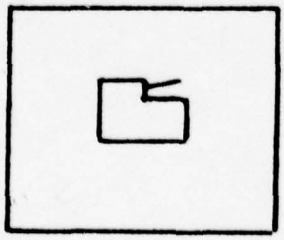

Figure 2.0-4 Track Window For
Disappearing Target

It is important, in the presence of obscuring pixels which may be at the same gray level as the target to obtain as clean a segmentation of the remaining portion of the target as possible. The purpose of this section is to sharpen the segmentation algorithms developed under the DARPA|NV & EOL Smart Sensor Program for a variety of FLIR target sizes for the case of small targets in the presence of obscurations and TV images as well. Performance figures for detection and classification for these algorithms have already been derived and it is not the intent here to modify those figures. The intent is to stay with the algorithm configurations already described for detection and classification and modify them only for tracking through obscurations. Hence the sharpening process has a rather narrow focus. The sharpening would be applied within the 16x16 track window in which the cuer may anticipate finding the target as handed back to it by the tracker. However, some effort must be devoted to minimizing false alarms within the 16x16 window due to the sharpening process.

The need for the sharpening process first appeared in Westinghouse work on the Pave Spike Program and appeared again on the NV & EOL TV data base and the Smart Sensor algorithms. It seems that a 5x5 Median Filter and a 4x4 Gradient Operator, where the Operator is as large as the target, acting on a 4x4 pixel target smears the edges. That is, the edge ramps are relatively narrow with respect to the operator. Hence an appropriate strategy is to reduce the operator size for this case.

2.1 Algorithm Review

A system flowchart of Smart Sensor algorithms is shown in Figure 2.0-5. In general, the Median Filter acts to suppress noise. The Gradient Operator extracts edges which are then thinned by the Non-Maximum Suppression Algorithm. At the same time a set of gray levels is determined and the filtered image is thresholded at each gray level. A Connected Components Algorithm partitions

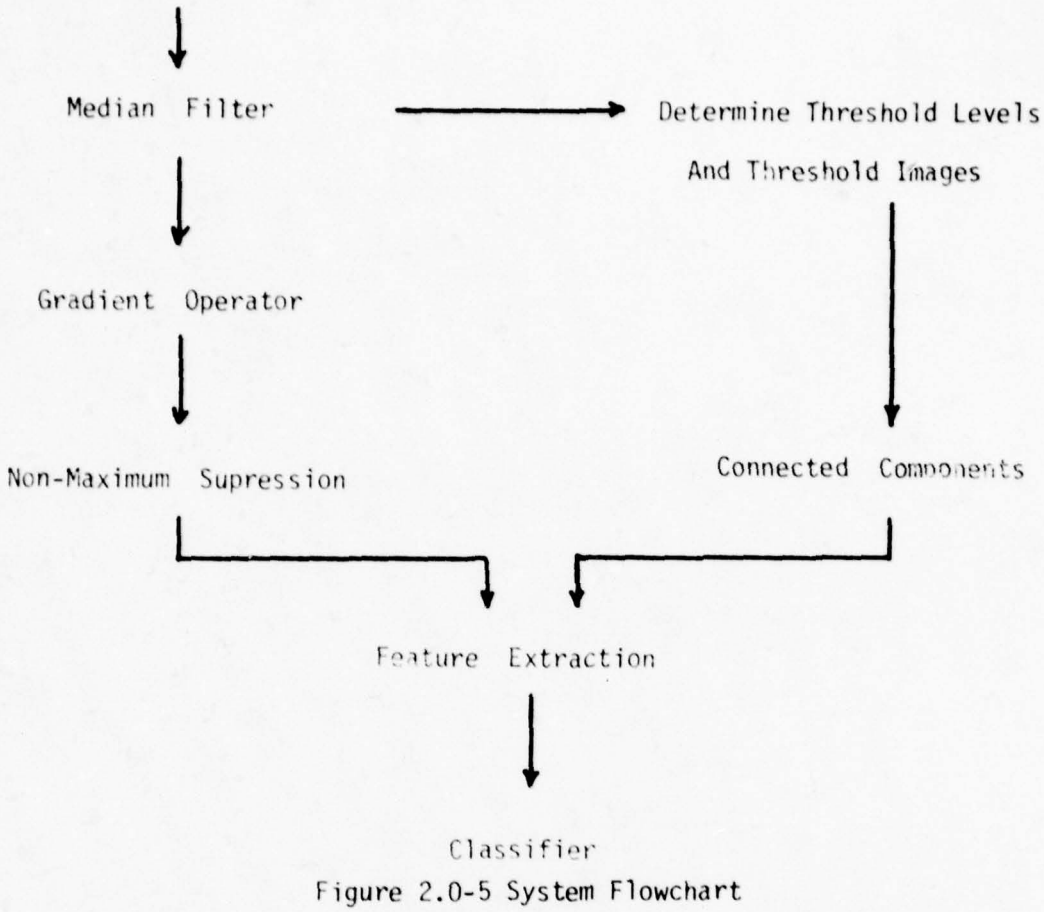

Figure 2.0-5 System Flowchart

each of the thresholded images into potential object regions. The Super Slice Algorithm correlates perimeter points formed independently by the Non-Maximum Suppression and Connected Components Algorithms and a score is obtained for each gray scale threshold. These scores and several other algorithms form a set of classification logic.

The Median Filter acts to extract the median value from a 5x5 pixel window moving across the image and place that value in the center pixel location of the window.

The Gradient Operator is an edge detector which is defined as GRAD OP = Max $\{|A-B|, |C-D|\}$ where A, B, C, and D each represent the sums of overlapping regions of 4x4 pixels each, as seen in Figure 2.0-6. The value of GRAD OP is placed in the pixel location marked "X" which is one pixel to the left and above the center of the entire region.

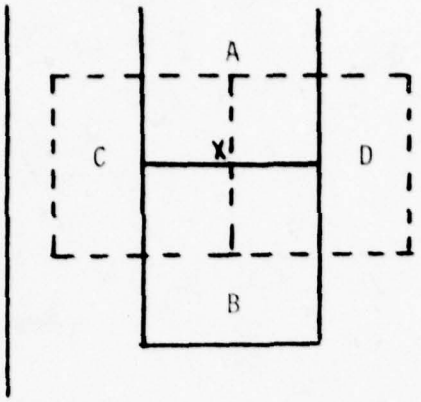

Figure 2.0-6 Gradient Operator

The Gradient Operator extracts edges in either the horizontal or vertical direction; the Non-Maximum Suppression Algorithm then looks in a direction perpendicular to the edge for a larger gradient. If a larger value cannot be found, the edge under consideration is retained; the edge is removed if a larger value is found. The algorithm is shown in Figure 2.0 -7.

```
x x x
x x x
  x
  y      →   Otherwise retain y
  x          x, y are gradient values
x x x
x x x
```

If any x>y, y = 0

Figure 2.0-7 Comparison Arrangement
for Non Maximum Suppression

2.2 A Sharpening Variation

The purpose of the sharpening variation is to enhance edge detections without increasing the false alarm rate in the 16x16 window. This is to be accomplished by reducing the window size in the algorithms which act to produce edges, namely

the Median Filter, Gradient Operator, and Non-Maximum Suppression. Reducing the Median Filter window not only increases the number of false edges in the window, but it produces a rather ragged looking target which exhibits more diagonal edges than before. Correspondingly, the extent of the vertical and horizontal edges are reduced. Another approach seemed to produce better results, namely a reduction in the Gradient Operator regions A, B, C, and D to a 2x2 each and a corresponding change in the Non Maximum Suppression Algorithm shown in Figure 2.0-8 for a horizontal edge. Since the edge ramps are more narrow for the smaller targets, the extent of the comparison neighborhood can be reduced.

```
x x x
          IF Y≥x, y=y
  y
          IF y<x, y=0
x x x
```

Figure 2.0-8 Non-Maximum Suppression

2.3 A Comparison

Figure 2.0-9a shows an image of an APC taken from the NV & EOL data set described in Section 5.0 after a 5x5 median filter was applied. The image has been thresholded at T=13 so that the gray levels less than or equal to 13 become 1's and the gray levels > 13 are 0's. Figure 2.0-9b is the corresponding Non-Maximum Suppression output for the 4x4 Gradient Operator and Non-Maximum Suppression mask described in Section 2.1. Figure 2.0-9c represents the same outputs for the algorithm described in Section 2.2.

```
17 17 17 16 16 14 14 14 15 16
16 16 16 13 13 11 11 12 14 14
16 13 12 11 10 10 10 11 12 14
16 13 12 11 10 10 10 11 12 14
16 13 13 12 11 11 12 16 19 20
18 18 18 18 18 19 20 21 21 22
```

Figure 2.0-9a 5x5 Median Filter for t≤13 Image 290

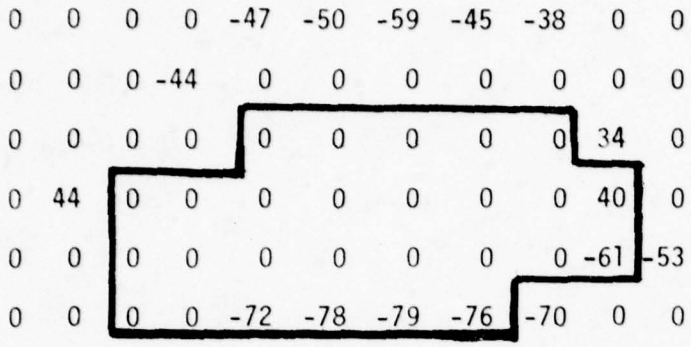

Figure 2.0-9b 4x4 Output

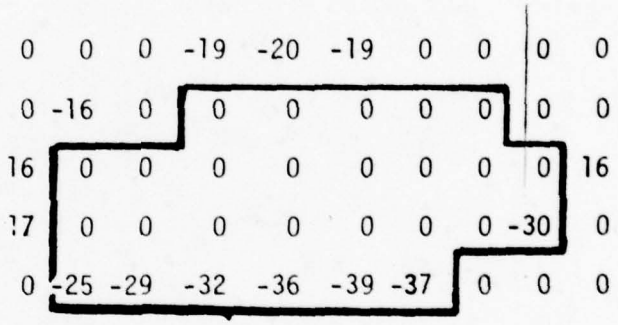

Figure 2.0-9c 2x2 Output

The 2x2 output has more edge definition along the top and the rear of the target which is moving from left to right. In fact the 2x2 output reaches a maximum number of matches at a lower threshold than the 4x4 case, thus yielding more compact targets with less danger of merging into the background on the left sides.

Figure 2.0-10a shows the blob for window 300 and threshold $T \leq 13$. Figures 2.0-10b and 2.0-10c show the edges remaining after Non-Maximum Suppression operations for the 2x2 and 4x4 Gradient Operators respectively. There is no

support on the left side for the 4x4 or 2x2 operators. The results for $t \leq 13$, 14, 15 are summarized in Table 1.

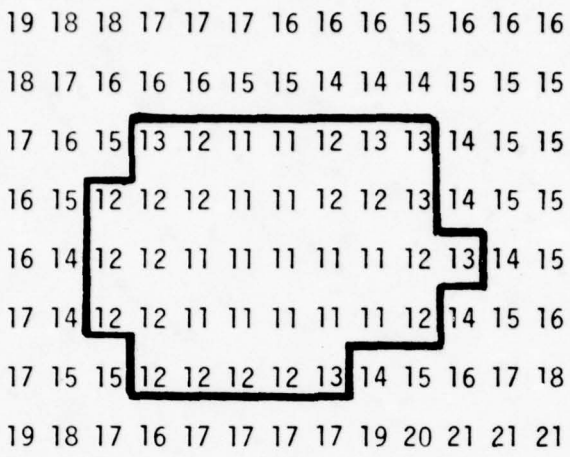

Figure 2.0-10a 5x5 Median Filter, Image 300, $t \leq 13$

The 2x2 Gradient Operator at $\tau \leq 14$ achieves a 66 percent parimeter match with 2 points or pixels supporting the left side, three points supporting the right, five points supporting the top and nine points supporting the bottom. This is more than the percent of matches achieved by the 4x4 at $t \leq 15$ and with two more edges supporting the right side.

0	0	0	0	0	0	0	0	0	-8	0	0	0
0	0	-15	-17	-19	-19	-15	0	0	0	0	0	4
0	0	0	0	0	0	0	0	0	7	0	0	0
13	0	0	0	0	0	2	0	0	0	0	0	0
15	0	0	0	0	0	0	0	0	10	0	0	8
13	0	0	0	0	0	0	0	0	0	0	0	0
0	0	0	-26	-28	-29	-29	-29	-29	-26	-23	-20	-18
0	0	0	0	0	0	0	0	0	0	0	0	0

Figure 2.0-10b. 2x2 Grad Op., 300, $t \leq 13$

-30	-35	-41	-46	-47	-47	-45	0	0	0	0	0	0
0	0	0	-46	-47	0	0	0	0	0	0	0	0
0	0	0	0	0	0	0	0	0	0	0	0	0
42	0	0	0	0	0	0	0	0	0	27	0	0
43	0	0	0	0	0	0	0	0	0	0	0	0
39	0	0	0	0	0	0	0	0	0	0	0	0
-35	-43	-52	-58	-62	-64	-65	-69	-61	-57	-52	-47	-43
0	0	0	0	0	0	0	0	0	0	0	0	0

Figure 2.0-10c. 4x4 Grad Op., 300, $t \leq 13$

Table I. Window 300

	GRADIENT	LEFT	RIGHT	TOP	BOTTOM	TOTAL	%	TOTAL
$t \leq 13$	2x2	0	2	4	7	13	57	(23)
	4x4	0	1	2	8	11	48	
$t \leq 14$	2x2	2	3	5	9	19	66	(29)
	4x4	2	1	2	11	16	55	
$t \leq 15$	2x2	3	2	6	10	21	64	
	4x4	3	1	5	12	21	64	

Figure 2.0-11a shows the blob for window 310 at a threshold of $t \leq 13$. Figures 2.0-11b and 2-11c show the edges remaining after non maximum suppression operation for the 2x2 and 4x4 gradient operators, respectively. The results for window 310 are shown in Table 2. At $t \leq 13$, the results are fairly even for the two gradient and non-maximum suppression masks. Further, the percentage of perimeter point matches is quite high, and the distribution of supporting edges seems adequately distributed. It appears that at $t \leq 13$, the 2x2 has a slightly better performance.

18	17	17	16	16	16	16	16	16	16	16	16
17	17	17	16	15	14	13	13	14	15	16	16
17	16	16	14	13	11	9	9	12	12	15	16
16	14	13	11	8	8	8	8	9	10	15	15
16	14	13	11	8	8	8	8	9	10	15	16
16	16	15	14	10	9	9	9	12	15	16	16
16	16	16	16	18	19	20	21	22	22	23	23

Figure 2.0-11a 5x5 Median Filter, 310, $t \leq 13$

0	0	5	0	0	0	0	0	0	0	0	0
0	0	0	0	-21	-23	-24	0	-18	0	0	0
0	-12	0	0	0	0	0	0	0	18	0	0
0	0	16	16	0	0	0	0	0	23	0	0
0	0	0	0	0	0	0	0	0	0	0	0
0	0	0	-30	-43	-48	-51	-50	-44	-36	-31	-29
0	0	0	0	0	0	0	0	0	0	0	0

Figure 2-11b. 2x2 Grad Op., 310, $t \leq 13$

0	0	-34	-42	-51	-58	-58	-54	-42	0	0	0
0	0	0	0	0	0	0	0	0	28	0	0
0	0	39	0	0	0	0	0	0	43	0	0
0	0	44	44	0	0	0	0	0	50	0	0
0	0	0	0	0	0	0	0	0	0	0	0
0	0	0	-63	-80	-95	-99	-98	-89	-78	-69	-61
0	-37	-49	0	0	0	0	0	0	0	0	0

Figure 2-11c. 4x4 Grad Op., 310, $t \leq 13$

Table 2. Window 310

	GRADIENT	LEFT	RIGHT	TOP	BOTTOM	TOTAL	&	PERIMETER POINTS
$t \leq 13$	2x2	2	2	4	7	15	68	22
	4x4	2	2	3	7	14	64	22
$t \leq 14$	2x2							
	4x4							
$t \leq 15$	2x2							
	4x4							

Figure 2-12a shows the blob for window 340 and $t \leq 13$. Figures 2-12b and 2-12c show the 2x2 and 4x4 Grad Op. results, respectively. The analytic results are shown in Table 3. Again the 2x2 is showing good support for each side and a high percentage of matches which can be approached by the 4x4 case by increasing the threshold level. Even though the number of support edges for each side may be smaller in the case of a lower threshold, recall that the object is also smaller so that the percent supported is approximately the same.

19	19	18	19	17	17	17	17	17	17	16	16	16
19	18	18	17	17	17	17	17	16	15	15	16	16
18	18	17	16	16	16	16	15	14	14	14	14	16
18	16	16	15	14	14	14	12	11	10	13	14	14
17	16	14	14	13	12	10	9	9	9	9	13	14
16	15	14	13	12	11	10	9	9	9	9	12	15
16	15	14	11	10	10	10	10	9	9	12	14	15
17	16	14	11	10	10	10	11	12	13	14	15	18
17	17	16	15	13	13	13	13	14	15	18	19	20
18	18	18	19	19	20	22	22	21	21	21	21	21

Figure 2-12a. 5x5 Median, 340, $t \leq 14$

0	0	0	0	0	0	0	0	0	0	0	0	0
0	0	0	0	0	0	0	0	0	0	0	0	0
0	-9	-9	0	0	0	0	-20	-21	-20	-17	0	0
9	0	0	0	0	0	0	0	0	0	0	0	0
0	0	0	0	0	10	0	0	0	0	18	18	0
0	0	0	-10	0	0	0	0	0	0	0	0	0
0	0	+17	0	0	0	0	0	0	0	0	0	0
0	0	0	0	0	0	0	0	0	0	-24	-19	0
-7	0	0	-29	-34	-39	-41	-36	-30	0	0	0	0
0	0	0	0	0	0	0	0	0	0	0	0	4

Figure 2-12b 2x2 Grad., 340 $t \leq 14$

0	0	0	0	0	0	0	0	0	0	0	0	0
0	0	0	0	0	0	0	-54	-53	-46	0	0	0
0	0	0	-37	-42	-47	-51	-54	0	0	0	23	0
0	0	0	0	0	0	0	0	0	0	0	34	0
0	0	0	0	0	0	0	0	0	0	42	42	0
0	39	0	0	0	0	0	0	0	0	0	46	0
0	37	37	0	0	0	0	0	0	0	0	0	0
0	0	0	0	0	0	0	0	-76	-70	-62	-52	-43
-24	-36	-46	-58	-72	-79	-83	-82	0	0	0	0	0
0	0	0	0	0	0	0	0	0	0	0	0	12

Figure 2-12c. 4x4 Grad., 340, $t \leq 13$

Table 3. Window 340

	GRADIENT	LEFT	RIGHT	TOP	BOTTOM	TOTAL	%	PERIMETER POINTS
$t \leq 13$ {	2x2	2	2	5	8	17	71	25
	4x4	1	3	2	8	14	58	25
$t \leq 14$ {	2x2	1	1	6	8	16	50	32
	4x4	2	4	6	10	22	69	32
$t \leq 15$ {	2x2							
	4x4	2	4	7	12	25	69	36

Figure 2-13a shows the blob for window 410 and $t \leq 13$. Figures 2-13b and 2-13c shows the non-maximum suppression results for the 2x2 and 4x4 Gradient Operator, respectively.

19	19	19	19	19	17	17	17	16	16	17	17
19	81	81	71	16	15	15	15	15	15	16	17
19	18	16	14	13	13	11	11	11	13	13	15
17	16	14	13	11	8	8	8	9	9	13	17
17	16	14	13	11	8	8	8	9	9	13	17
16	15	14	13	11	8	8	9	16	18	19	20
17	16	16	16	16	18	18	19	20	21	22	22

Figure 2-13a. 5x5 Median, 410, $t \leq 13$

0	0	0	0	0	0	0	0	0	0	0
0	-16	-20	-22	-24	-26	-24	-20	0	0	0
13	0	0	0	0	0	0	0	0	0	0
0	0	16	16	0	0	0	0	24	24	0
0	0	16	16	0	0	0	0	-36	0	0
0	0	0	-35	-44	-46	-42	0	0	0	0
0	0	0	0	0	0	0	0	0	0	0

Figure 2-13b. 2x2 Grad Op., 410, $t \leq 13$

-24	0	0	0	0	0	-56	-47	-33	0	0
0	-38	-49	-58	-64	0	0	0	0	0	0
0	41	0	0	0	0	0	0	40	0	0
0	47	0	0	0	0	0	0	51	0	0
0	0	0	0	0	0	0	0	0	0	0
0	0	0	0	-87	-92	-89	-83	-71	-61	-53
0	-53	-66	-76	0	0	0	0	0	0	0

Figure 2-13c. 4x4 Grad Op., 410, $t \leq 13$

Table 5 shows the results for image 410 as applied to both of these gradient operators. Again, the 2x2 shows a higher percentage of matches for lower thresholds and the 2x2 exhibits a more even distribution of supporting edges. There is no need to continue with the remainder of Table 5. In summary, the

2x2 gradient, through a small set of examples, has generally shown a higher percentage of matches and a more even distribution of supporting edges.

Table 5. Results for Window 410

	GRADIENT OP	LEFT	RIGHT	TOP	BOTTOM	TOTAL	%	PERIMETER POINTS
$t \leq 13$	2x2	4	3	5	6	18	90	20
	4x4	2	2	3	8	15	75	20
$t \leq 14$	2x2							
	4x4							
$t \leq 15$	2x2							
	4x4							

In conclusion, this work indicates that the 2x2 case does produce better edge definition than the 4x4 case, for this set of images. For very noisy images, the smaller window is suspect and will produce edges which may show good coincidence. On the other hand, the 5x5 Median Filter has been retained to reduce the spurious signals in a low signal to noise ratio image. We shall adopt the 2x2 Gradient Operator and corresponding Non Maximum Suppression Mask for tracking in the case of obscurations within the 16x16 window. Further quantitative results will indicate how well the sharpened preprocessor algorithm is performing.

3.0 FRAME TO FRAME TRACKER

In Section 1.0 and 2.0, we discussed a number of factors affecting the design of the frame to frame tracker. Simultaneous, multiple target tracking of 15 or so targets puts a premium on tracker speed and hardware. To produce these kinds of speeds and target handling capability, a simple tracker such as a binary correlation tracker is appropriate. This places more reliance on the cuer preprocessing functions for segmentation and also demands a closer interaction between cuer and tracker in the form of an addressable frame storage device divided into horizontal strips. If a more powerful tracker is needed such as a bandpass binary correlation tracker, then the cuer must provide frequent updates to the bandpass. If more cooperation between cuer and tracker is necessary the small window, high update rate cuer may be implemented and/or we may move to more sophisticated trackers such as gray level correlation. The strategy then is to take full advantage of cuer presence to simplify the frame to frame tracker in order to boost its speed and target handling capability because in all three scenarios it seems likely that multiple target tracks will be established and maintained before classification and prioritization are completed. Further, in the AAH case, multiple target track points will serve as a basis for reacquiring targets which have left the field of view because of their own movement or the movement of the sensor.

In the following paragraphs, we discuss a number of technical aspects of the tracker, namely a description of the baseline frame to frame tracker which provides the initial design start, a variation which is applicable to the close-in homing case, additional computations for aimpoint selection at long range, a track window position update strategy, and an example of binary correlation tracking as applied to the NV&EOL data base.

3.1 Baseline Frame to Frame Tracker

The baseline tracker described in this report has been programmed and exercised on the 525 line TV data base as supplied by NV&EOL. Initially, the cuer is used to "seed" the tracking process, i.e. the cuer defines a region of the field of view which contains the desired target. Size data concerning the target is employed to generate a set of nested regions about the target as shown in Figure 3.0-1. The size of the inner window is chosen such that at least

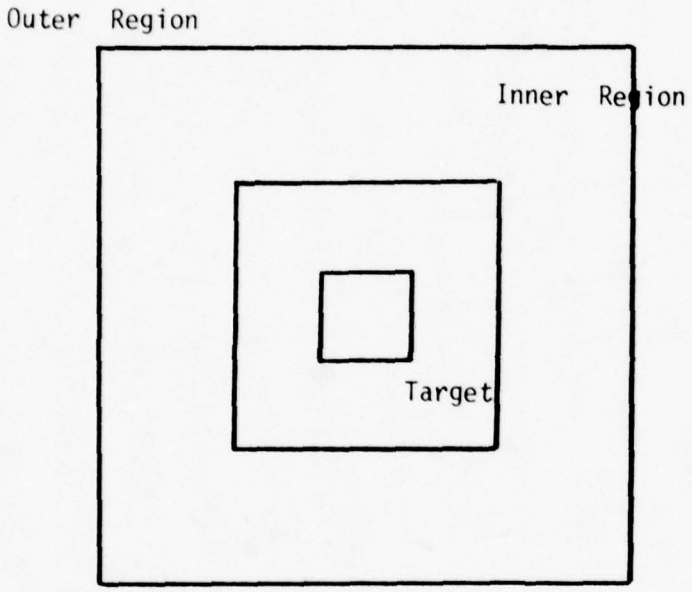

Figure 3.0-1 Nested Regions

90 percent of the target is enclosed. The outer region is twice the linear dimension of the inner one. For the RPV case, for example, the 4x4 pixel target would require a 5x5 pixel inner window and a 10x10 pixel outer window. The next step of the processing is to generate gray level histograms for each of the mutually exclusive regions. Let p_{ij} be the pixel sample value

for the pixel occurring at row i, column j relative to the top left hand corner pixel of the outer region. Then define

$$Q_{ij}^{k} = \begin{cases} 1 & \text{if } p_{ij} = k \\ 0, & \text{otherwise} \end{cases}$$

where k is the gray tonal value of the pixel. The histogram for the outer and inner regions (HO and HI, respectively) are formed by summing the patterns defined by Q_{ij}^{k} for every possible gray level, $k \in [o, g_{max}]$, where g_{max} is the largest value allowed by the video digitization process.

$$HO(K) = \sum_{i} \sum_{j} Q_{ij}^{k} \qquad ,ij \in O$$

$$HI(K) = \sum_{i} \sum_{j} Q_{ij}^{k} \qquad ,ij \in I$$

This histogram information is then used to define the gray tones which are unique to the target. This is accomplished by forming a positive difference function PD for all tones:

$$PD(K) = \begin{cases} |HI(K)-HO(K)| & \text{if} > 0 \\ 0 \quad \text{Otherwise} \end{cases}$$

Note that the difference is taken between the corresponding gray level counts for the inner histogram and the outer (annulus) histogram. Next a discriminant function, D(k), is formed. In the most basic algorithm D(k) is set to one for those gray levels, K, for which the positive difference function is non zero. Other variations are possible. The most successful one involves using the histogram and positive difference function data to define a passband of gray levels such that

$$D(K) = \begin{cases} 1 & T_L \leq K \leq T_H \\ 0 & K < T_L, \quad K > T_H \end{cases} .$$

The threshold values T_L and T_H are chosen such that the number of target gray levels is maximized while the number of background gray tones is minimized in the passband.

Once the discriminant function has been derived, a binary image, $\hat{P}$, is created from the original pattern, P, according to the transformation defined by the discriminant function

$$\hat{P}_{ij} = D(P_{ij})$$

This preprocessed pattern, $\hat{P}$, serves as an input for the track algorithm. The tracking algorithm originally stores an nxn reference array, R, of binary pixels. The dimensionality, n, is determined by the cueing algorithm according to the size of the detected target. On subsequent frames, the image is preprocessed into a binary pattern according to the acquisition discriminant. NXN subarrays of the preprocessed pattern are exclusive - ORed with the original reference array, R, on an element by element basis. The result of this logical operation are summed over all elements to define a track metric, Crs, i.e.

$$C_{rs} = \sum_{i=1}^{n} \sum_{j=1}^{n} S_{r+i-1,\, s+j-1} \oplus R_{ij}$$

The coordinates r,s define the coordinates of the subarray with respect to some common reference point, typically the upper left hand corner of the image roster. The track metric, C_{rs}, is computed for several different subarrays. The exact number is dependent upon the initial target dimensionality. For example, if n = 8, all track metrics for the 81 possible subarrays within a 16x16 window about the present target position are computed. The location of the minimum value for the track metric is used to define the new track point and the tracker error. This is relayed to the cuer for future reference and can also be used to stabilize a sensor and/or designator upon the target. For cases where the target is much larger, e.g. n = 16, a directed

has left the field of view. These quantities also serve to point the cuer to that portion of the image in which the target was last seen. The multiple target track function requires that the track point and tracker error be computed for all the detected targets in the image. The target track could also be used to insure that the cuer and tracker are both working on the same target. For target signature prediction as described in Section 2.0, the track error is overridden and the window is positioned such that the rear portion of the target is centered in the track window. By using the cuer to initially center the window and size the window, the probability of including other targets within the inner track window is diminished.

3.2 A Variation for Close-in Homing

The cuer is assumed to locate the track window such that the desired target is centered in the region. Within the track window two concentric windows are constructed, as shown in Figure 3.0-2. The track window is shown as 0, the next window is labelled M, and the inner window is labelled C. Depending on the target size, the dimensions of the windows may have to be adjusted.

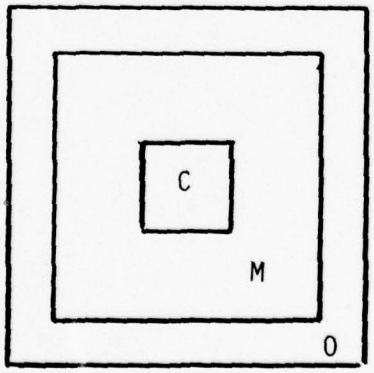

Figure 3.0-2 3 Windows

The preprocessor forms the histogram of gray scale for each of the window segments, as shown in Figure 3.0-3.

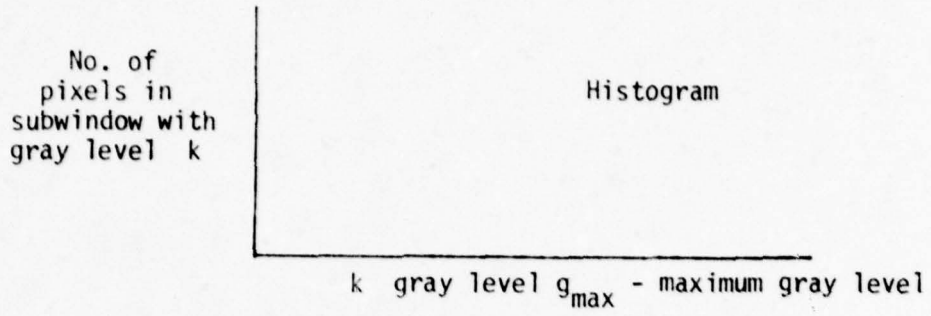

Figure 3.

Let $$Q_{ij}^{k} = \begin{cases} 1 & P_{ij}=k \\ 0 & \text{Otherwise} \end{cases}$$

then $$HO = HO(K), \quad K=1,2,\ldots g_{max}$$

where $$HO(K) = \sum_i \sum_j Q_{ij}^{k} \qquad ij \in O,\ ij \notin C,M$$

Similarly, the histograms for the other windows are defined as:

$$HM(K) = \sum_i \sum_j Q_{ij}^{k} \qquad ij \in M,\ ij \notin C,O$$

and

$$HC(K) = \sum_i \sum_j Q_{ij}^{k} \qquad ij \in C,\ ij \notin M,O$$

The windows are sized such that the target is almost completely enclosed within the middle window M. The difference between this approach and the former is the anticipation for close-in homing. The inner window will allow us to track on a particular feature within the target outline. Next,

window pairs are measured for content. We define a window content measure as follows.

$$M_{MC} = \sum_K M_1(K) \quad \text{where} \quad M_1(K) = \begin{cases} HC(K) - HM(K) & \text{if} > 0 \\ 0 & \text{Otherwise} \end{cases}$$

$$M_{OM} = \sum_K M_2(K) \quad \text{where} \quad M_2(K) = \begin{cases} HM(K) + HC(K) & \text{if} \geq 0 \\ 0 & \text{Otherwise} \end{cases}$$

The measure of window content will determine which set of histograms to use to derive the preprocessing transformation.

If

$M_{OM} \geq 4\ M_{MC}$ choose pair O,M

Otherwise, choose the inner window set. Once the proper window pair has been picked, the function M(K), either M_1 or M_2 depending on the test outcome, is used to define the preprocessor, i.e.

$$M(K) = \begin{cases} M_1(K) & \text{if } 4\ M_{MC} > M_{OM} \\ M_2(K) & \text{if } M_{OM} \geq 4\ M_{MC} \end{cases}$$

Define a discriminant function D(K).

$$D(K) = \begin{array}{ll} 1 & M(K) > 0 \\ 0 & M(K) \leq 0 \end{array}$$

The raw video pixels are then transformed into binary pixels according to the discriminant function.

$$\{P_{ij} = D(P_{ij})$$

This defines a binary pattern which represents the pixel characteristics of the gray levels of the target. There are other possible preprocessing transformations. This transformation from raw gray levels to binary patterns is one of the more simple ones and will be used for the first phase of the investigation. It may turn out that this variation of the baseline tracker is employed after the highest priority target has been selected and close-in homing initiated. It is applicable to the PGM scenario where the range to impact is 1500 meters or less. Prior to these conditions for the PGM scenario and the AAH and RPV scenarios the baseline tracker may suffice. At 1500 meters or less the maneuverability may be limited to such an extent, that tracker "dither" is the paramount problem, i.e. the aimpoint wandering around the target.

3.2.1 Track Computations for Aimpoint

There appears to be two tracking algorithms suitable for use in the Intelligent Tracker, centroid and correlation. They can be applied to any input pattern (raw video, binary, preprocessed linear video). Centroid tracking is accomplished by computing the centroid on the preprocessed pattern, if it is preprocessed,

$$\bar{X} = 1/U\left(\sum_i \sum_j j\, p_{ij} \right) \qquad \bar{Y} = 1/U\left(\sum_i \sum_j i p_{ij} \right)$$

where

$$U = \sum_i \sum_j p_{ij}$$

Other useful quantities are the spatial variances,

$$\epsilon_x^2 = 1/U \left(\sum_i \sum_j j^2 p_{ij} - \bar{x}^2 \right) \qquad \epsilon_y^2 = 1/U \left(\sum_i \sum_j i^2 p_{ij} - \bar{y}^2 \right)$$

Although we will not use centroid tracking in the initial phases, because it is suspect in heavy clutter, we shall be computing the centroid and spatial variances which will be used in aimpoint selection.

3.3 Update Strategy

On frames between times when the cuer produces a target, the correlation track algorithm is executed. The raw image is preprocessed according to

$$\hat{P}_{ij} = D(P_{ij})$$

in the region defined by the track window, say 32x32 for this example. This region is searched for the point of best correlation of the initial, e.g. 16x16 reference with the 16x16 subregions of the preprocessed track window. The starting coordinates of a 16x16 subregion, with respect to the first pixel of the track window is called a search center. Figure 4 illustrates this. For each member, a set of search centers $\{r,s\}$ a correlation number is computed. Thus, the starting pixel of the subwindow defined by search center r,s is $\hat{P}_{r+1,\ s+1}$. Note that the center window

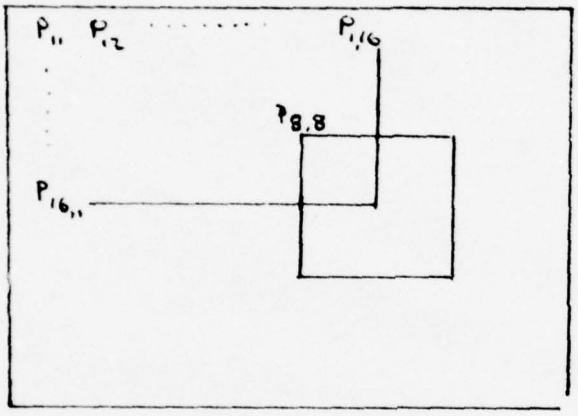

Figure 4.

has search center 8,8. The correlation number is computed for each search center in the set r,s according to

$$C_{rs} = \sum_{i=1}^{16} \sum_{j=1}^{16} \left| P_{ij} - P_{r+i-1,s+j-1} \right|,$$

The track point is derived from the minimum correlation number

$$C_{r^* s^*} = \{C_{r\ s}\} \quad .$$

The strategy of selecting search centers is now described.

The track error in whole pixel units is determined from the minimum center according to

$$\Delta X = s^{\star} - 8, \quad \Delta y = r^{\star} - 8$$

Once the track error has been found two things can happen.

1. The errors Δx, Δy are used to drive the servo so as to keep the target centered in the track window.
2. The track window is moved in the raster to follow the target; this is called in active track.

Because of the nature of the study, we shall be employing the latter, the track window position is modified for the next frame to be

$$l' = l + \Delta x \qquad k' = k + \Delta y$$

Note, that if the cuer provides target information, the location provided by the cuer overrides the correlation returned error.

The current search strategy is a three phase process. Phase I involves looking for the minimum correlation number for a set of fixed values given in Table I. The phase one correlation minimum location serves as the starting point of the phase 2 search. Table II gives offsets for the phase 2 search centers with respect to the phase I minimum. Once the phase II minimum is located, it may still be the phase I minimum, phase III is started.

Table I. Phase I Fixed Search Centers

r (row coord.)	s (column coord.)
2	2
2	6
2	10
2	14
4	4
4	8
4	12
6	2
6	6
6	10
6	14
8	4
8	8
8	12
10	2
10	6
10	10
10	14
12	4
12	8
12	12
14	2
14	6
14	16

Table II. Offsets with Respect to Phase I Min.

r (two coord.)	s (column coord.)
-2	0
+2	0
0	-2
0	+2

Table III gives these offsets with respect to the minimum location at the end of Phase 2. The search center with the minimum correlation value at the end of Phase 3 defines the new track point.

Table III. Offsets with Respect to Phase II Min.

r (row coord.)	s (column coord.)
0	+1
0	-1
+1	0
-1	0
-1	-1
-1	+1
+1	-1
+1	+1

3.4 Application of the Baseline Tracker

The purpose of this section is to demonstrate that the baseline tracker is working with the NV & EOL data base and the output format. As an example of the baseline tracker applied to the NV & EOL data base, we selected a set of six consecutive frames from the data base described in Section 5.0. Figure 3.0-5 shows a plot of the approximate xy positions of the target taken from the digital printout of the video tapes for consecutive frames 245 through 250.

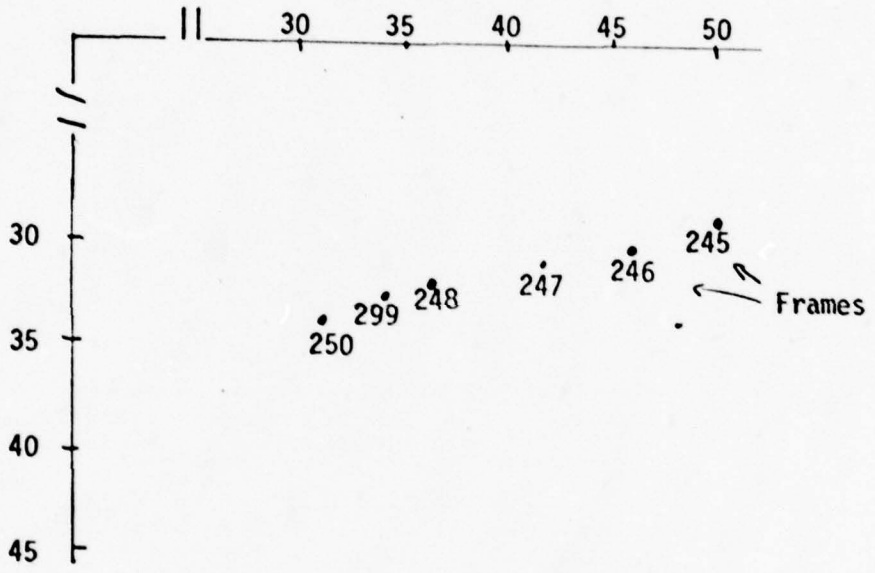

Figure 3.0-6. xy Plot of Target Positions

The 16x16 window is shown in Figure 3.0-7, and the inner window is also drawn. The histograms are computed for each window and the PD function is shown in Figure 3.0-8. The Positive Difference (PD) function shows the gray levels, derived from the histograms, which are unique to the target and is shown in Figure 3.0-8.

27	27	26	26	25	25	25	25	25	25	25	25	26	26	26	26
28	27	27	26	26	26	25	25	25	25	25	25	26	26	26	26
27	27	26	26	26	26	25	25	25	25	25	25	25	15	26	27
27	27	26	26	26	25	25	25	25	25	25	25	25	18	25	26
26	26	26	25	25	24	21	21	21	20	21	22	23	24	25	27
26	25	25	24	23	21	20	18	18	18	18	19	21	22	23	25
25	25	24	22	21	18	17	14	14	14	17	17	19	21	22	24
25	24	23	21	17	16	12	11	12	12	14	15	17	19	21	24
24	23	22	20	17	16	12	11	12	12	14	15	17	19	21	24
24	23	22	21	18	17	16	12	12	13	14	16	19	20	21	22
24	23	23	22	21	17	17	17	17	18	19	19	20	21	22	22
25	25	25	23	23	21	21	21	21	21	21	21	22	22	22	22
25	25	25	25	25	24	24	23	23	23	22	22	22	22	23	23
26	26	25	25	25	25	25	25	24	24	24	24	24	24	23	23
26	26	26	26	26	26	26	25	25	25	25	25	25	25	26	24
26	26	26	26	26	26	26	26	26	26	26	26	26	26	26	26

Figure 3.0-7 Inner and Outer Windows

0	1	2	3	4	5	6	7	8	9	10	11	12	13	14	15	16	17	18	19	20	21	22

Figure 3.0-8 Positive Difference Function

The gray levels unique to the target are 11, 12, 13, 14, 15, 16, 17, and 21. Then the reference image for the 8x8 window according to PD is shown in Figure 3.0-9. The reference is correlated against itself and the resulting image, centroid calculations for aimpoint, and correlation computations as shown in Figure 3.0-10.

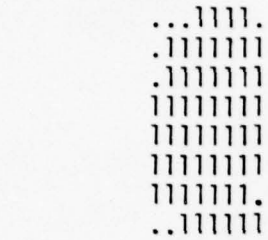

Figure 3.0-9 Reference Image

Figure 3.0-10 First Window Computations

R and S are the horizontal and vertical track errors for a given correlation value C. The image at the upper left is the new reference image based on the correlation, and $\bar{X}$, $\bar{Y}$, SIG2X, SIG2Y etc. are the centroid computations of mean, spatial variances and so on for the image shown. Figures 3.0-11 and 3.0-12 show the new reference image, track errors, and centroid computations for images 246 and 247.

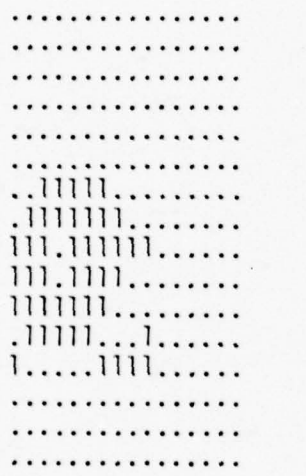

XBAR = 5.836
YBAR = 9.936
SIG2X = 34.468
SIG2Y = 102.106
SIGXY = 52.489
THETA = .499

DELX = -5 DELY = 1

IMAGE NUMBER = 246

Figure 3.0-11 Image 246

YBAR = 4.389
YBAR = 9.889
SIG2X = 24.944
SIG2Y = 102.704
SIGXY = 44.426
THETA = .426

DELX = -4 DELY = 1

IMAGE NUMBER = 247

Figure 3.0-12 Image 247

The conclusions based on this test is that the tracker is working on the NV & EOL data base, but the track errors have room for improvement. We plan

next to try a band pass correlation tracker over those same images to see if performance can be improved. Further, the search technique for the minimum needs improvement because in image 246 and 247, the next to minimum value was chosen thus contributing to the window offset. Another measure of increasing complexity to be tried in the sequence of more complex trackers is gray level correlation.

4.0 TARGET SIGNATURE PREDICTION

The purpose of this section is to describe preliminary efforts of target signature prediction in the presence of obscurations in order to support a tracking strategy. The work is described in terms of an analysis of three scenarios from the NV&EOL data base. Several hypotheses are put forward for the individual cases. At this point a general thread or theory is not apparent, although the goal is certainly to avoid allowing the target signature prediction problem to degenerate into a number of special cases.

A more general problem associated with target signature prediction is a determination of the level at which the problem is attacked. For example, is it necessary to identify roads, woods, fields, shrubs and so on in order to perform target signature prediction? Considering the practical aspects of the matter, i.e. the scope of this contract and the state of the art in identifying roads, woods, fields, etc., as exemplified by the DARPA Image Understanding Program, we think that approach is ambitious. Instead, we will avoid that approach and concentrate on the level at which the problem is difficult for a tracker standing alone. An example mentioned in a recent paper[1] is one in which the target approaches an obscuration at approximately the same gray level as the target, the target becomes obscured, and then moves away while the tracker remains locked on the obscuration. Consider the three scenarios and the hypotheses suggested for each.

4.1 Road Crossing Case

The scenario has an APC starting in a field to the left of a road, moving across the road, and continuing into the field on the other side. A window from the initial portion of the scenario is shown in Figure 4-1.

1. Assessment of Target Tracking Techniques, Capt. B. Reischer, paper 178-06 Proceedings of SPIE, Volume 178, Smart Sensors, April 17-18, 1978.

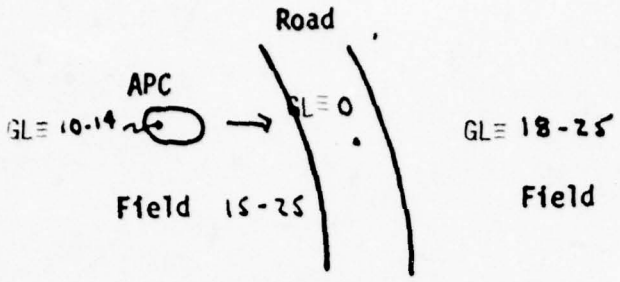

Figure 4-1. Road Crossing Case

A rough estimate of the gray levels for the initial window is also shown in Figure 4-1. As opposed to images analyzed in prior studies ,e.g. the DARPA/NV&EOL Smart Sensor work, this set of images offers changing polarities for the same target. That is to say, the APC in Figure 4-1 is initially represented as a light target against a dark background. When the APC is straddling the left shoulder of the road, the rear portion of the target is represented again as a light target against a dark background. However, the front portion of the target on the road is represented as a dark target against a light background. When the target straddles the right shoulder, the front and rear portions of the target reverse polarities with respect to their respective backgrounds. To illustrate this point, consider the set of images in Figures 4-2a,b, and c. In Figure 4-2a, the image has been thresholded from low gray levels and every pixel <14 is labelled as a 1; every gray level >14 is not labelled. When the target is straddling the

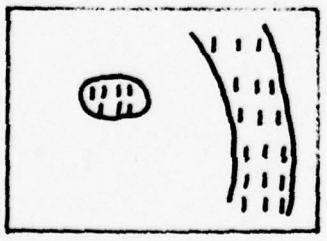

Figure 4-2a. $T \leq 14$

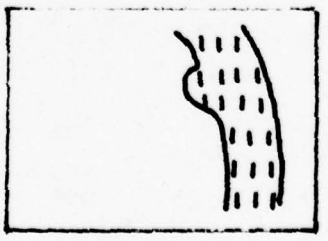

Figure 4-2b. $T \leq 14$

left shoulder of the road, as shown in Figure 4-2b, a clean segmentation of the target cannot be obtained. If we slice down from the highest gray levels, the same result is obtained, as shown in Figure 4-2c, with the road and target appearing as a "hole". This is, they are part of the unlabelled region.

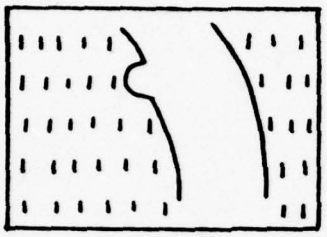

Figure 4-2c. T >14

There are several approaches to this problem, e.g. 1) tracking the target by tracking target shadows or internal contrasts which are separable from the background, 2) bandpass segmentation similar to techniques discussed in the tracker section, 3) change detection, 4) reliance on edges rather than gray levels for segmentation, and 5) others. In this Quarterly, we consider 1) and 5); approaches 3) and 4) are considered in later work.

4.1.1 Use of Interior Contrasts and Target Associated Regions

An example from the NV&EOL data where the first of these approaches is useful is shown in Figure 4-3 in which the shadow of the previous target has been noted.

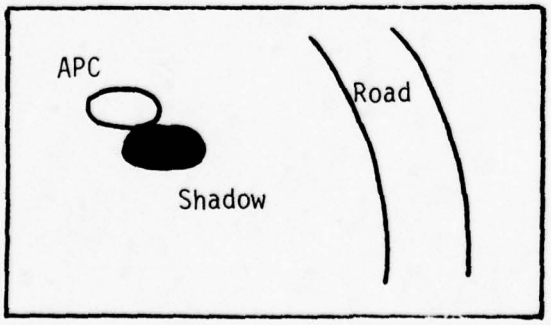

Figure 4-3. Shadow Present

The shadow is composed of gray levels 25-30 and is clearly visible as the target crosses the road. We could track the shadow instead of the target and the problem reduces to one of tracking a dark target (the shadow) across a background which varies in gray level but is always lighter than the target (shadow) and hence a clean segmentation is always possible. However, before arriving at this nice position, there are several interesting issues to be settled. Is the dark region a part of the target (e.g. cold or dark part of an otherwise hot or bright target), associated with the target but not part of it (e.g. shadow of the vehicle, dust, or smoke plume due to target motion), or a part of the background (e.g. clump of shubbery, muddy spot on the ground, etc.)? This must be determined in order to decide whether it should be tracked and how to use the tracking data. We begin by assuming that the classification logic has correctly identified the APC in the initial images, Figure 4-3, and has not included the dark object as part of the APC. The next hurdle is to identify the dark object as something in the background (e.g. bush, mud patch, etc.) or something associated with the target (e.g. shadow, dust plume, etc.). For this classification, we may use features such as comparison of the sizes of the APC and dark object and the movement of both. There are problems with these features because target associated regions change with conditions (e.g. shadow change with lighting change, plume change with vehicle speed and ground surface conditions). For the movement feature, the target will have to move some minimum amount to determine whether or not the dark object is moving with the target. If the dark object is not moving with the target, then it is probably part of the background. Let us tabulate the x and y components of a vector centered in a coordinate system located in the APC according to the geometry of Figure 4-4, where the vector is drawn from the center of the APC to the center of the shadow. The displacements in x and y are shown in Table 1 over a selected set of frames in which the target has moved 24 pixels.

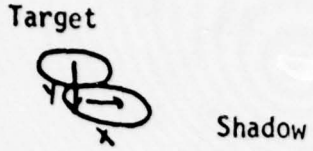

Figure 4-4. Target/Shadow Geometry

Table 1. Target/Shadow Displacement

FRAME NO. 1	y DISPLACEMENT	x DISPLACEMENT
1	-5	+2
2	-6	+5
3	-5	+5
4	-5	+6
5	-5	+3
6	-5	+3
7	-5	+3
8	-5	+3
9	-4	0
10	-4	+2
11	-4	+1
12	-6	+2
13	-6	+2

An examination of the table shows that the x and y components are constant with respect to a target movement of 24 pixels, thus indicating that the dark object is associated with the target. Another feature mentioned for determination of existence of an associated region is the relative size of the target and dark object. These are tabulated in Table 2 for the same sequence of frames. These data indicate that the sizes are relatively constant during the 24 pixel movement of the target. We may speculate that the dark object is approximately equal to size of the target, but under different conditions the size relationship might be quite different. Probably, the stability over time of the ratios of target and dark area sizes is the best indication we can hope for without attempting to account for the detailed conditions (e.g. sun angles, soil moisture,

Table 2. Target/Dark Object Dimensions

	TARGET		DARK OBJECT	
FRAME NO.	X Ext	Y Ext	X Ext	Y Ext
1	11	6	16	2
2	11	6	18	3
3	13	6	16	4
4	11	6	16	4
5	10	5	17	6
6	10	6	16	5
7	11	6	17	5
8	13	6	15	4
9	15	5	17	3
10	17	4	14	4
11	13	4	15	4
12	12	5	16	4
13	15	5	18	5

wind direction, etc.). An attempt to account for such conditions is well beyond the scope of the present effort and is probably not desirable in a real time tracker in any case.

Before leaving this line of analysis, let us digress for a moment and consider the case of attempting to classify a target which has distinct light and dark parts in order to obtain the correct classification we originally assumed. Suppose that the background is such that each portion of the target can be cleanly segmented. Because each is treated as a separate object, classification is not possible. However, as seen from Table 1, movement and a computation of the x and y components of a vector joining their centers can provide reasonable evidence that the objects are moving together. Conceivably, these portions could be joined in a Connected Components sense and classification logic successfully applied to the combination.

In conclusion, we have analyzed the road crossing case from the standpoint of tracking objects or areas associated with or part of the target. This is an important special case because environmental conditions are not always favorable but it seems that such techniques may be required in any case in order to correctly classify targets with strong internal contrasts.

4.1.2 Other Approaches

Another approach to the road crossing case where a clean segmentation appears unlikely is to determine and use a band of gray levels which are characteristic of the target only. To obtain the band, we follow the usual procedure of successive slices $gl \leq T_1$, $gl \leq T_2$, ... and match edge points with perimeter points to obtain the maximum number of matches. Then, the gray levels representing the target are considered to be in the band. For example, the band of gray levels 10-14 characterize the target in Figure 4-1. There are areas to be investigated in this approach also, because we found that the band of gray levels representing the target changes as the background changes. For example, the maximum gray level on the front part of the target when that portion is on the road is 8. Hence, the band cannot be set at 10-14 and never updated, but must be adaptive. Previously, we spoke of the changing target polarity with respect to the background; the problem also contains the element of changing gray levels within the target. In conclusion, a band of gray levels may be useful if the change in the band can be predicted.

We will consider this problem further in the next Quarterly as well as several other approaches involving change detection and detections relying more on edges such as can be found in one mode of the Westinghouse Auto-Q System. Another idea is to shift the tracker to the rear of the target when it straddles the left shoulder; the rear of the target has a predictable bandpass here. While the rear is tracked, frame to frame, the cuer is looking for the emerging front end on the raod. Having found it, the tracker is shifted to the front

end. In this approach, the idea of obtaining a clear segmentation of the entire target is discarded.

4.2 THREE TARGETS CROSSING CASE

The scenario is an APC passing between two stationary APC's as shown in Figure 4-5. All three APC's are roughly at the same intensity (gray) levels so the question of adaptive bands is not relevant. As the target on the left closes with the other two, their respective shapes merge prohibiting a clean

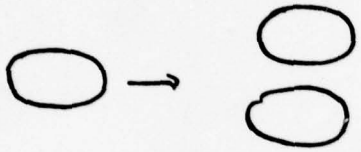

Figure 4-5. Crossing APC's

segmentation of the targets and also obliterating target outlines as shown in Figure 4-6. The problem is to separate the targets. In this kind of situation (as opposed to the road which extends from the bottom of the window to the top), it is possible to track the y coordinates of the targets. The y coordinates are interesting because they can be used to determine which target is in front

Figure 4-6. Merged Targets

of the other. For example, the y coordinate of the bottom of each target in Figure 4-5 indicate that the left APC is passing behind the lower APC and in front of the upper APC. Figure 4-5 is redrawn as Figure 4-7 with the y coordinates added; y_{1t} is the coordinate of the top of target 1, and y_{1b} is the coordinate of the bottom of target 1, and so on.

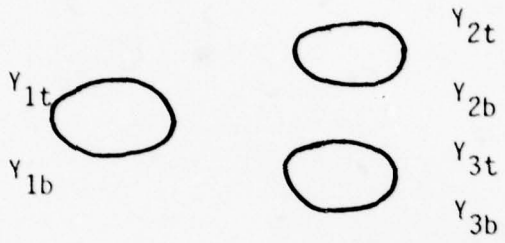

Figure 4-7. Crossing Targets, y Coordinates Added

These coordinates can be computed and tracked on every cued frame. Further, we establish a file by vertical position such that, since $y_{2t} > y_{1t} > y_{3t}$, it is ordered 2,1,3. Table 4 shows a track of these coordinates as the left target crosses the other two and emerges. In the first four frames there is

Table 4. y Coordinates for Three Targets

FRAME NO.	y_{1t}	y_{1b}	y_{2t}	y_{2b}	y_{3t}	y_{3b}
1	47	50	41	44	49	56
2	45	50	41	44	49	54
3	21	24	16	20	25	32
4	27	32	24	28	33	40
5			49			64
6			55	64	67	72
7			87	94	97	104
8	26	33	24	30	34	39

still a separation between the targets. The coordinates are varying from window to window because the TV sensor is not on a stabilized platform. However, if we used differences between y coordinates the perspective information is maintained as shown in Table 5. In frames 5 through 7, there is merging so the middle

Table 5. Perspective Track

FRAME NO.	$y_{2t} - y_{3b}$
1	15
2	13
3	16
4	16
5	15
6	17
7	17
8	15

dimensions do not have much meaning. If the left target passes between the other two, then $y_{2t}-y_{3b}$ must remain fairly constant as shown in Table 5. Since the merging occurs in the middle of the three, we shall be tracking the rear portion of the left target, the top portion of the top target, and the bottom portion of the lower target.

There is another phenomena observed in these images and is something we shall call bridging. When the targets come within a few pixels of each other, bridges begin to form between them as illustrated in Figure 4-8. That is,

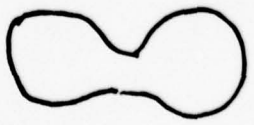

Figure 4-8. Bridging

the gradient from the light target to the darker background in its usual decay by another bright object. This is probably caused by the limited MTF of the

sensor and oversampling in the video digitization which combine to produce the "mixed pixels" which form the bridge. The significance of this observation means that, if there is a shape merging, clean segmentations will be limted when they are within a few pixels of each other. This implies that the look ahead window must be of the order 5 to 7 pixels.

4.3 FADING TARGET

This scenario has an APC moving through a thick woods at long range so that the target is only a few lines high on some frames and perhaps six lines high on others. Further, the shape is changing between frames; this problem is accentuated by the TV camera not being mounted on a stabilized platform and the fact that the camera is being panned. Our first approach to this problem will be to test to see if it indeed is a problem or whether tracking is possible without signature change prediction. In short, it will provide an interesting case for the baseline tracker. Recall, that we are following the strategy of using a relatively simple tracker in order to achieve the speeds and target handling capability demanded by the multiple track function. If the simple tracker can handle the fading target case, and can handle target signature prediction in conjunction with a cuer, confidence in this overall apprach will be increased.

4.4 SUMMARY

Study of the problem of predicting and continuing track through changes in target signature has begun by considering three cases from the NV&EOL data base where such approaches may be important. That is, we have selected cases where the simple frame to frame tracker can expect to fail and the cuer may have difficulty distinguishing the target(s). Although target signature change prediction would seem to eventually depend upon identification of major non-target image areas (e.g. roads, woods, fields) such a high level of automatic image understanding is beyond the current state of the art and is

deemed beyond the scope of this contract. Nevertheless, several interesting and potentially productive research issues have been noted in this area. Broadly, these all depend on generating a more thorough automatic analysis of the details of the target signature itself. This may include analysis of the interior target contrasts, regions associated with (genertd by) the target which are not part of it (e.g. shadows, dust, plumes, tracks), better separation of target and background intensity regimes, analysis of the target by portions (e.g. front or rear) and analysis of foreground/background relationships between segmented objects. Further investigation of these areas is critical to understanding the basis for more robust target cueing, critical aimpoint analysis, and multi-target tracking and this work will continue and be expanded in the next quarter.

5.0 NV&EOL DATA BASE

The purpose of this section is to describe the NV&EOL TV data base supplied under this contract. A description of the FLIR portion of the data base was provided in the first quarterly. The index number for each tape segment refers to the length meter on a Sony tape recorder. This may vary for the reader's case depending on how much tape is used in the threading operation. Nevertheless, the index should be within ±25 of the meter on the reader's 525-line tape machine.

5.1 Tape C 1,3

Tape Position 0001

The jeep and truck are dark targets on one side of the light road and the 3 APC's are light targets on the road. There is a light strip of ground parallel and to the right of the road. Initial position of the vehicles is shown in Figure a. The vehicle geometry after some movement is shown in Figure b. Initial acquisition is at medium to long range. There is substantial merging of target shapes.

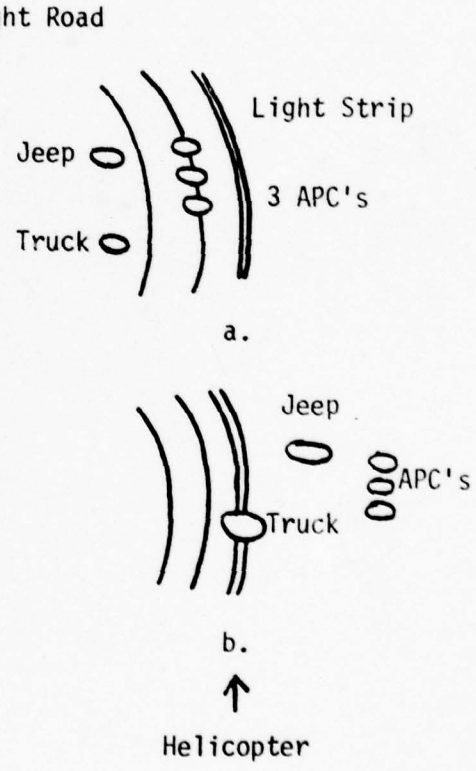

Tape Position 0044

The jeep and truck have reversed positions with each other and the two vehicles stay together. Acquisition range is longer and the helicopter altitude seems to be higher than in 0001. Initial Vehicle positions are shown in Figure a. and after some elapsed time, the vehicle positions are shown again in Figure b. Even at the higher altitudes the target shapes merge part of the time.

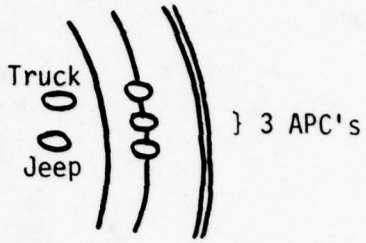

a.

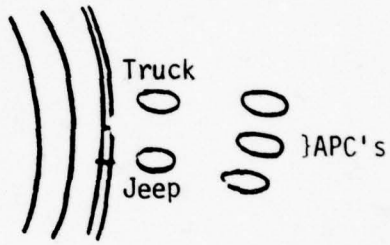

b.

↑
Helicopter

Tape Position 0092

Initial vehicle positions are shown in Figure a. Here the truck starts on the road with the jeep on the shoulder. The 3 APC's are well off the road. The lower helicopter altitude is responsible for a significant amount of shape merging. The vehicles stay together, while moving, in two separate groups as shown in Figure b. This section ends with the helicopter flying over the targets which is true for all these runs.

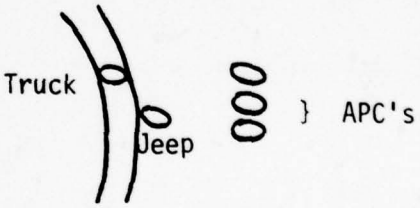

a.

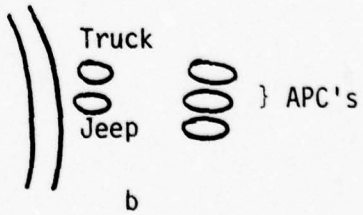

b

↑
Helicopter

Tape Position 0123

Initial acquisition is at long range with the vehicles placed along the border of a woods. The vehicles are stationary and appear light against the gray field and darker woods. Four of the target shapes are merged, with the leftmost APC standing alone.

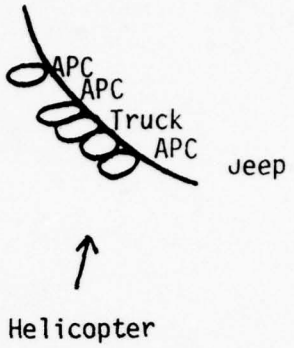

Tape Position 0153

A repeat of tape position 0123, at a greater helicopter altitude and medium acquisition range.

Tape Position 0198

The run geometry is same as 0153, but the vehicles have been changed. The truck standing alone is a pick-up truck as seen from the rear and the other truck is a military troop truck. One of the APC's has been removed and replaced with a tank.

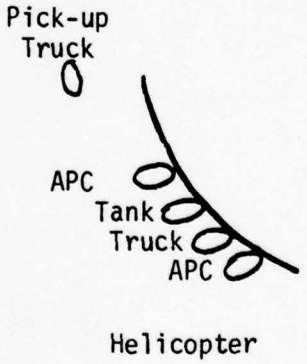

Tape Position 0218

A repeat of tape position 0198 with acquisition at medium range. The sensor then swings away from the stationary target along the woods and follows the truck moving on the road.

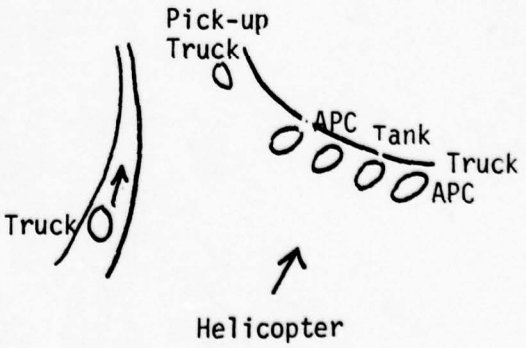

Tape Position 233

A repeat of 0198 with acquisition at medium range; the run is terminated before the helicopter flies over the targets. The altitude appears to be greater than that of tape position 0198.

Tape Position 248

The same target geometry as tape position 0198 but the acquisition range is longer and the helicopter azimuth apprach angle appears to be different. The run finishes with the helicopter flying over the targets.

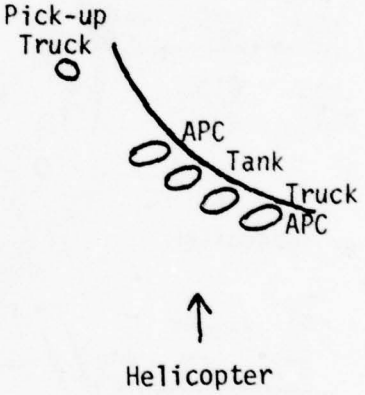

Tape Position 0273

The tank has a light top and dark treads and appears to the left of the road. The truck and jeep are dark targets to the right of the road, and the two APC's appear as light targets. All the targets are stationary.

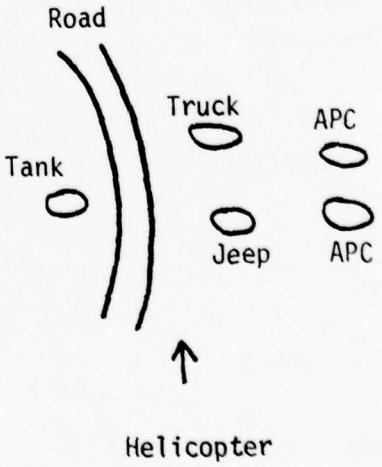

Tape Position 0290

Same target geometry as tape position 0273; here the tank moves across the road and between the other targets. The run ends when the tank passes between the truck and jeep.

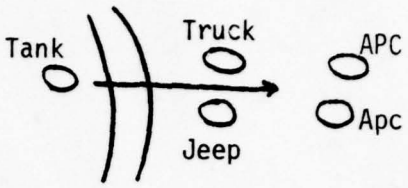

Tape Position 0307

Same run geometry as 0290, except that the tank starts on the other side of the road. The tank passes between both pairs of targets.

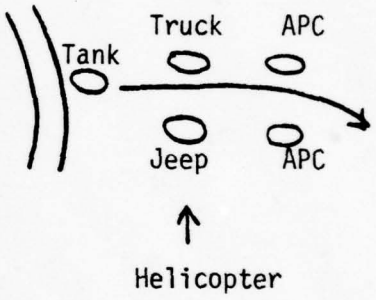

Tape Position 0323

A repeat of 0307 except the acquisition range is long and the altitude is lower. A front view of the tank is also shown. There is more shape merging in this run because of the helicopter position.

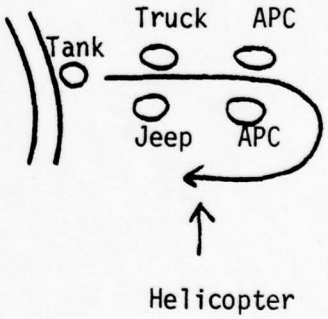

Tape Position 0344

A repeat of 0307.

Tape Position 0359

The tank starts from the left side of the road and passes between the two pairs of targets. There is shape merging and the mud to the right of the road blends in with the lower portion of the tank.

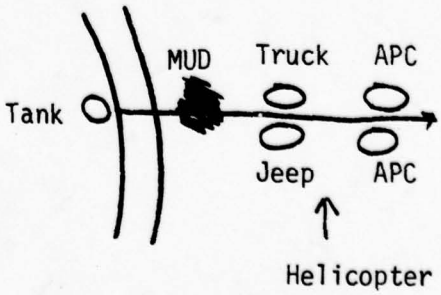

Tape Position 0378

A repeat of 0359 except that the helicopter flies over the tank just after it emerges from the APC's.

Tape Position 0394

Close range of tank moving around a curve in the road. As the tank rounds the curve, it is obscured by trees and only a small portion of the tank is seen.

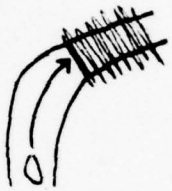

Tape Position 0410

A jeep and tank are moving along a road. The trees along the side of the road provide partial obscurations as the targets pass by.

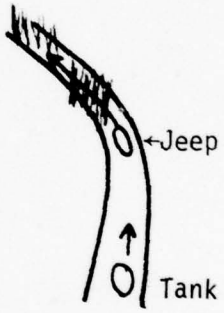

Tape Position 0417

A light tank is placed on a light road. The tank moves off the road through a scrub woods and then into a clearing as the helicopter flies over.

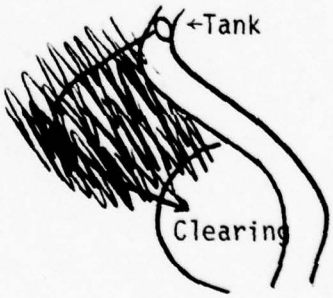

Tape Position 0443

A close range shot of tank moving on a road toward the helicopter.

Tape Position 0450

A tank is moving on a shoulder of the road and is lightly screened by trees in the foreground. Acquisition range is short.

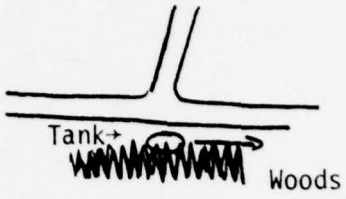

Tape Position 0459

A dark tank is moving on the dark shoulder of a road and generating a light plume behind it. The tank passes the jeep as the helicopter flies over.

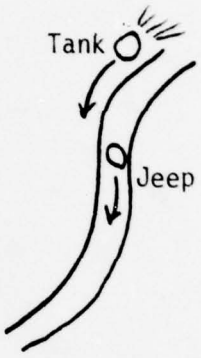

Tape Position 0468

A jeep and tank are moving in the same direction; the jeep is on the road and the tank is moving on the shoulder. As the jeep passes the tank, the tank goes into a gully and disappears from view. The tank reappears and the targets merge again after they move out of the curve in the road. A close range shot of a tank with a trailing dust cloud is seen at the end.

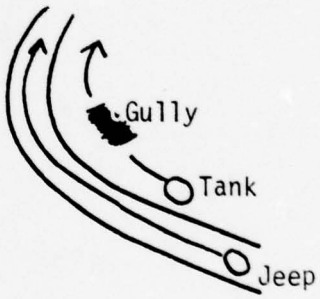

Tape Position 0481

A tank is moving on the shoulder of a road and toward the helicopter. A jeep is keeping pace with the tank but moving on the road.

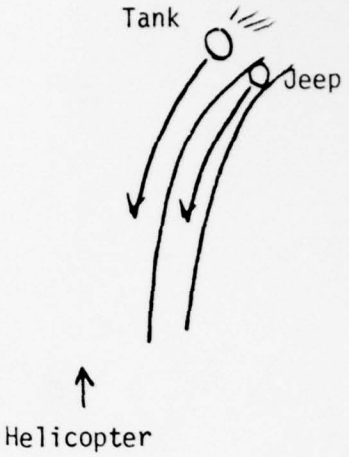

Tape Position 0488

The helicopter is following closely behind the tank seen in the foreground. In the background a jeep is seen moving along a road.

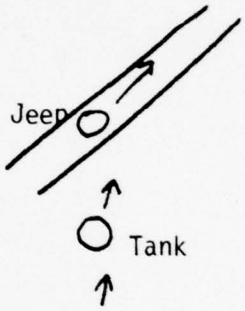

Tape Position 0494

A short range, side view of a tank moving at high speed. The helicopter then swings behind the tank showing a rear aspect.

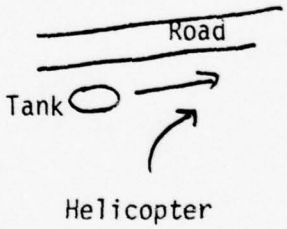

Tape Position 0498-0503

A front quartering aspect of a tank with a training plume is seen. The target is moving at high speed and the range is close.

Tape Position 0555-0566

Three stationary targets in an open field. The APC appears as a light target and the other two appear darker.

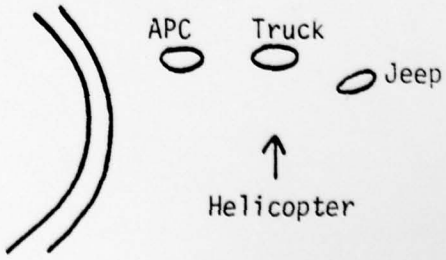

Tape Position 0573

APC is passing in front of the other two stationary targets; some limited shape merging with truck.

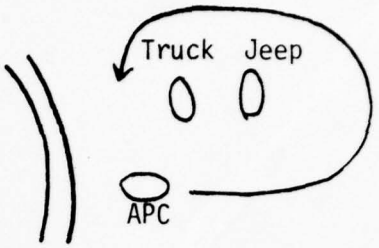

Tape Position 0588

APC circles the other two vehicles and then executes a circle between them with more shape merging. Run ends with APC heading toward helicopter as it passes overhead.

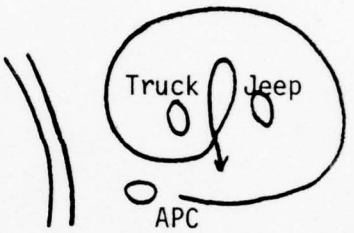

Tape Position 0605

Three targets, initially at long range, are approaching helicopter. The three targets are moving on parallel paths.

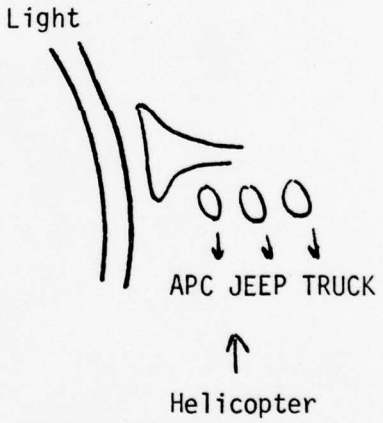

Tape Position 0630

Same run geometry as 0605, but this time the APC is the only target.

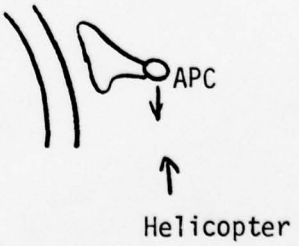

Tape Position 0665

Same run geometry as 0605 except that acquisition range is longer and positions of the targets have been changed.

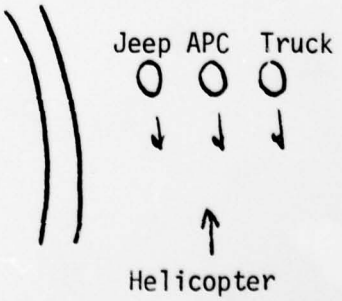

Tape Position 0684

APC is moving along edge of woods; it is a light target against dark woods and gray field.

Tape Position 0706

Close range image of dark truck moving along a light road. APC is then seen moving along shoulder.

Tape Position 0733

Close range images from quarter-rear aspect of a truck and APC moving in parallel. Run ends with close range rear aspect of APC.

Tape Position 0746

Medium and close range images of the side aspect of a moving APC are seen.

Tape Position 0770-0831

This section of tape contains repeated runs over the same target geometry shown in the figure. The targets are stationary and appear in the same geometry in each run.

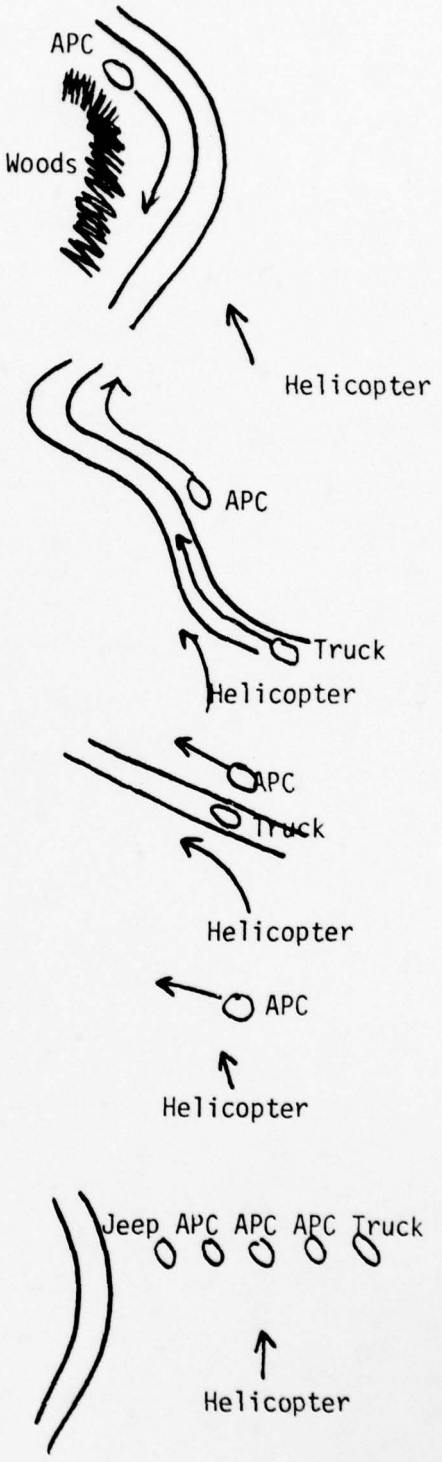

5.2 TAPE C_2

Tape Position 0030

Acquisition is obtained at recognition range on five stationary targets in an open field. The jeep appears as a dark target. The two APC's next to it appear as light targets. The truck and left most APC appear to have light and dark portions. The helicopter closes to about half the acquisition range and the run ends.

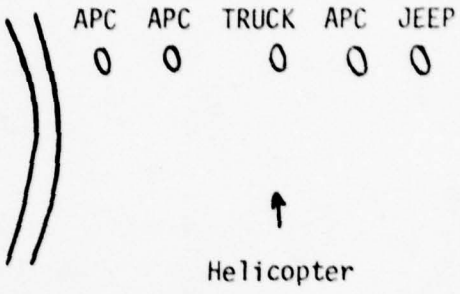

Tape Position 0052

A repeat of tape position 0030 with the range much shorter at the end of the run.

Tape Position 0076

This run has the same target and run geometry as 0030 except the acquisition occurs at long range. The range is long enough to cause shape merging. The helicopter altitude also appears to be greater.

Tape Position 0102

A repeat of run and target geometry as 0076 but at a higher altitude.

Tape Position 0136

This run has the same target geometry as the previous one but acquisition occurs with only 2 or 3 lines on the targets. As the helicopter closes it is also dropping in altitude, thus simulating a munition.

Tape Position 0192

Acquisition occurs at long range and the three targets to the left appear as one. The top target (APC) then moves to the left and then between the other two pairs of targets.

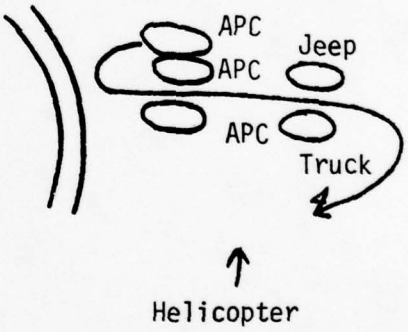

Tape Position 0240

The same target geometry as 0192 except here the APC crosses the road after going between the two pairs of targets and goes between both pairs a second time. The run ends with the APC between the jeep and truck for the second time.

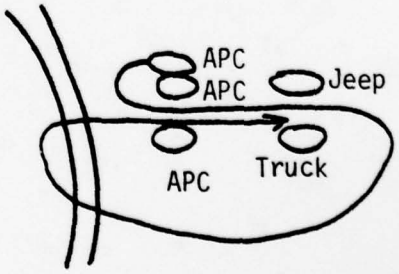

Tape Position 0293

Acquisition occurs at long range and the moving APC is to the left of the road. The helicopter altitude is quite high at the end of the run.

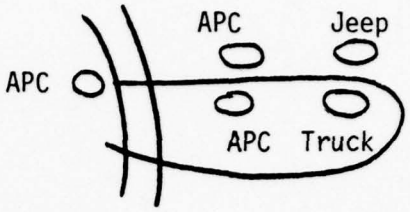

Tape Position 0326

Acquisition occurs at long range but the helicopter closes rapidly so that it flies over when the moving APC is between the other two APC's.

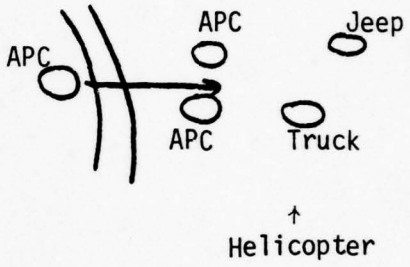

Tape Position 0351

Same stationary target geometry as the previous runs on this tape. Here, the moving APC starts from the road and passes between the truck and jeep by the time the helicopter passes overhead. The run ends with a close range, side view of the moving APC.

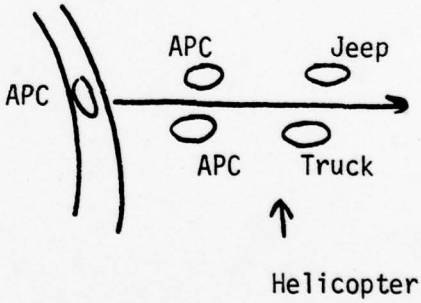

Tape Position 0377

Same target geometry as in the previous runs. Here, the APC starts from left side of the road and the helicopter flies over as the moving APC emerges from among the two APC's. Initial acquisition occurs at long range.

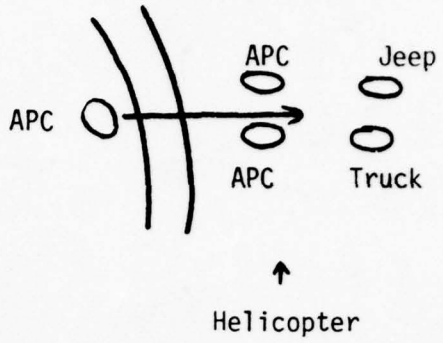

Tape Position 0449

Initial acquisition is obtained at medium range. Three stationary vehicles a jeep, APC, and truck are positioned in a clearing in a wooded area. An APC moves across the clearing and is partially obscured by the APC and truck. The APC stops before it enters the woods.

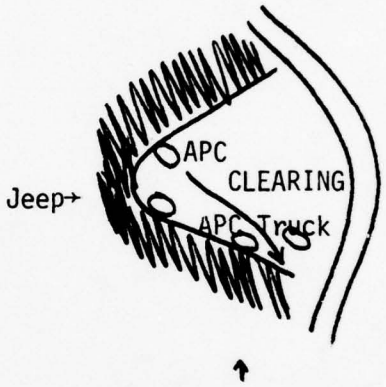

Tape Position 0463

A repeat of the stationary target geometry of 0449, but here the moving APC starts on the road. Initial acquisition is at longer range, but the APC does not begin to move until the range has close to medium. The run stops at approximately the same place as 0449. There is obscuration both with the other targets and with the scrub brush in the clearing.

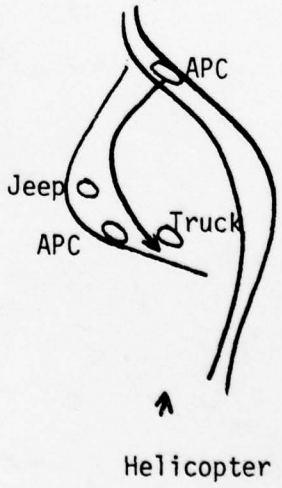

Tape Position 0473

A repeat of the previous target geometry. Here the APC starts at the edge of the clearing and passes among the other targets. It then moves among the woods until it approaches and moves onto the road. Acquisition is at medium to long range. The APC is partially obscured by the woods as it moves through them and back toward the road.

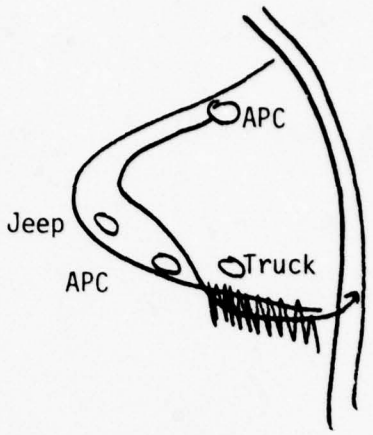

Tape Position 0493

Initial acquisition is obtained at long range with the moving APC on the road, the stationary target positions are the same as before. Again, the APC moves from the clearing into the woods resulting in a series of partial obscurations.

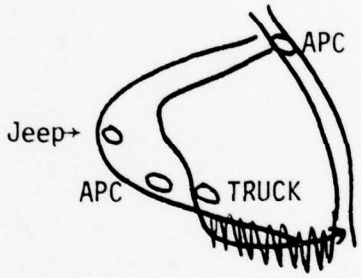

Tape Position 0504

A repeat of 0493 except that the APC moves between the APC and truck and then stops.

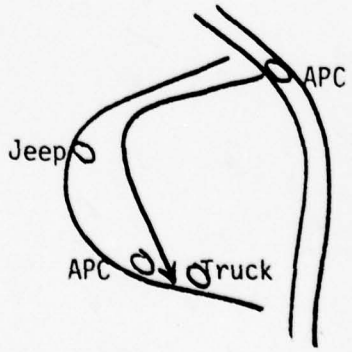

Tape Position 0521-0522

Initial acquisition is at long range. APC is positioned at the upper, left portion of the clearing. All the targets are stationary.

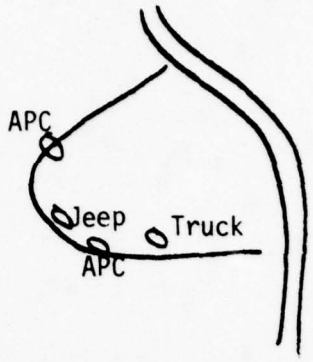

Tape Position 0531

A repeat of 0521 except that the APC begins to move when medium range is obtained. APC moves to a point between the APC and truck and stops. Helicopter flies over the targets.

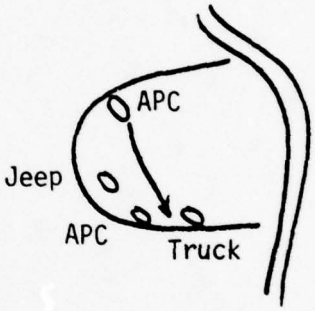

Tape Position 0545

Initial acquisition is at long range with the same stationary target geometry as before. The moving APC starts from the wooded area above the clearing. The run ends at approximately medium range as the APC enters the clearing.

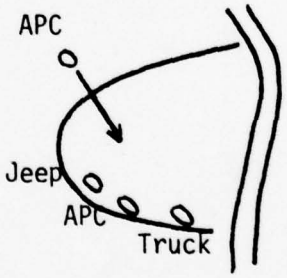

Tape Position 0560

A repeat of the stationary target geometry of 0545. The APC starts from the woods as in 0545, but does not begin moving until the helicopter has closed to medium range. Initial acquisition is at long range. The helicopter closes on the moving APC simulating a munition and flies over when the APC is abreast of the jeep.

Tape Position 0588

There are three vehicles stationary on a road. The road just ahead of the vehicles is screened by trees. Initial acquisition is at long range. As the helicopter closes, the truck moves up the road and behind the trees. The truck stops on the right side of the road. Then the APC moves behind the screen of trees along the left side of the road and stops ahead of the truck. The jeep then follows the APC and stops behind it. Both the APC and jeep stop in front of the truck.

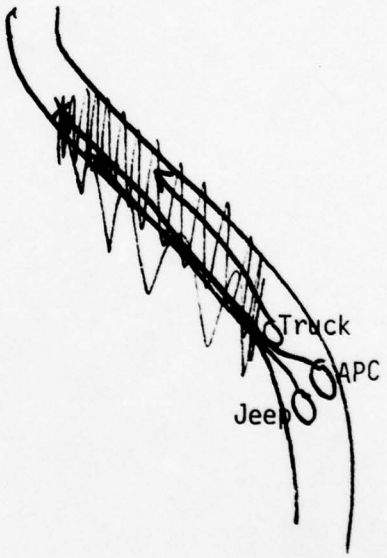

Tape Position 0612

Four targets are moving from the wooded area into the clearing. Scattered portions of them are seen as they move through the woods. The helicopter flies over the targets at the end of the run. The runs start with the helicopter at long range.

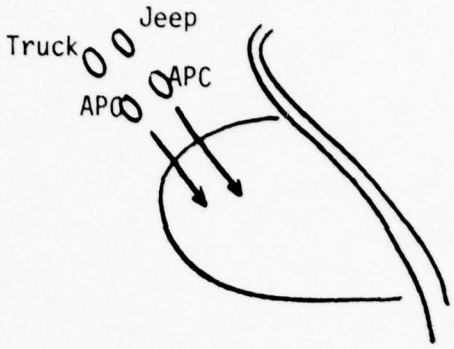

Tape Position 0655

The run begins with the helicopter at long range. The four targets are in the same arrangement as 0612 but the APC is positioned in the woods just off the clearing. As the helicopter approaches to medium range, the targets move into the clearing. The run ends when the targets have moved across the clearing.

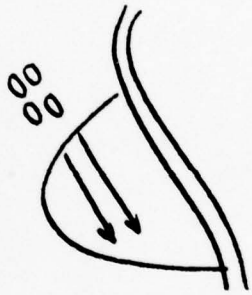

Tape Position 0674

A repeat of 0655 except the targets remain stationary until the helicopter has closed to short range.

Tape Position 0694

A repeat of 0655 target geometry but the helicopter comes in low, simulating a munition. The low closing angle causes the moving targets to be partially occluded by the scrub trees and brush in the clearing.

Tape Position 0706

Initial acquisition is at long range. A single APC is moving through the woods and scattered portions are seen. As it enters the clearing, it is travelling at high speed and turns in the direction of the approaching helicopter which is simulating terminal homing. The APC enters the woods before the helicopter flies over thus partially obscuring it.

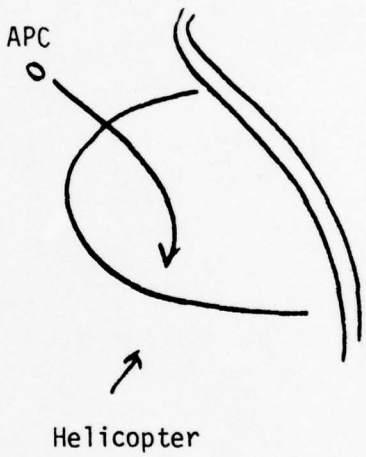

Tape Position 0716

A pair of APC's are moving through the wooded area and disappear from view. Initial acquisition is at long range. The APC's reappear again at the edge of the clearing and at a much shorter range.

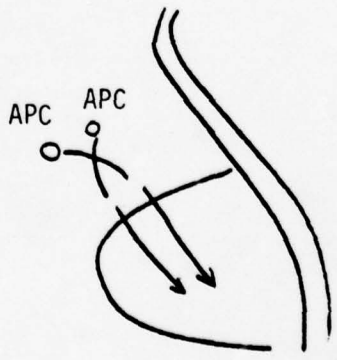

Tape Position 0729

Three targets start toward the clearing from well back in the woods. The run starts at long range. When the targets reach the edge of the clearing, they stop. After a short time interval, they move across the clearing as the helicopter closes.

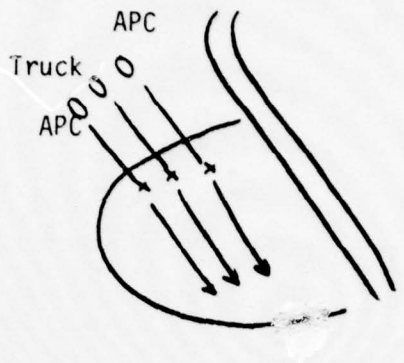

5.3 Tape C_4

Tape Position 0016

Helicopter approaches four stationary targets which are placed on the edge of a woods. The targets are close enough to each other that their shapes merge. At long range the APC's appear as light targets and the jeep and truck appear as dark targets. The hatch on the APC between the jeep and truck is up and the hatch on the other APC is down. At closer range, the targets have distinctive light and dark segments.

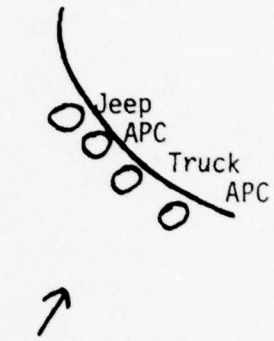

Tape Position 0052

A repeat of the target geometry of 0016, but it appears that the helicopter approach angle has been changed.

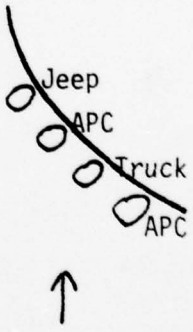

Tape Position 0084

Same geometry as 0052, but initial acquisition is at longer range and the helicopter altitude during the run is greater.

Tape Position 119

Same geometry as 0084 but acquisition is at medium range and helicopter appears to hover at short range. The helicopter does not fly over the targets.

Tape Position 0155

Same run and target geometry as 0016; acquisition is at long range. The helicopter flies over the targets for the first time on this tape and could simulate a homing munition.

Tape Position 0184

Acquisition is at long range with the three lower targets stationary. the APC in the upper part of the figure is barely visible and also stationary. When the helicopter has closed to approximately mid range, the APC begins moving. The helicopter seems to slow its approach almost to a hover as the APC moves. The helicopter does not fly over the target but maintains a stand-off range.

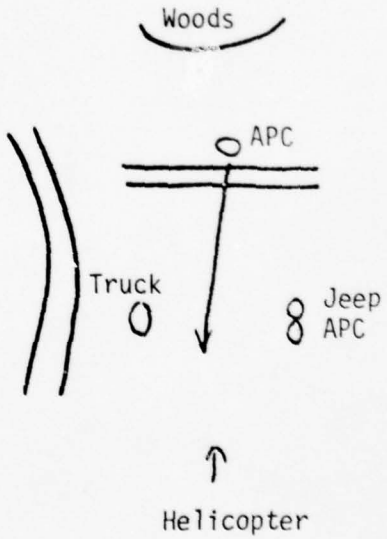

AD-A077 869 WESTINGHOUSE DEFENSE AND ELECTRONIC SYSTEMS CENTER B--ETC F/G 17/5
INTELLIGENT TRACKING TECHNIQUES.(U)
APR 79 T J WILLETT

DAAK70-78-C-0167

UNCLASSIFIED

NL

2 OF 2
AD A077869

END
DATE FILMED
1-80
DDC

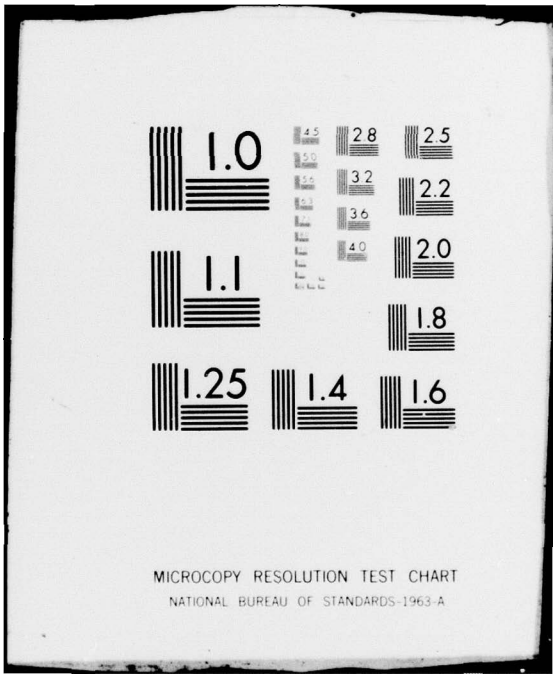
1.0
1.1
1.25
1.4
1.6
1.8
2.0
2.2
2.5
2.8
3.2
3.6
4.0
4.5
5.0
5.6
6.3
MICROCOPY RESOLUTION TEST CHART
NATIONAL BUREAU OF STANDARDS-1963-A

Tape Position 0221

A repeat of 0184 target geometry, except that the APC begins moving at acquisition which is at long range. The helicopter seems to hover at long range so the APC passes between the other vehicles at long range. The helicopter then closes and passes overhead.

Tape Position 0245

A repeat of 0221, except that acquisition range is longer. The APC repeats the maneuver of passing between the other targets.

Tape Position 0268

A repeat of 0245 except the altitude appears greater and the stand-off range is longer.

Tape Position 0289

Same stationary target geometry except the APC starts from the edge of the woods above the road. Acquisition is at long range and the helicopter loses altitude as it approaches, simulating a munition. The helicopter flies over while the APC is between the other vehicles.

Tape Position 0310

A repeat of 0289, except that the moving APC will be well past the other targets when the helicopter flies over it.

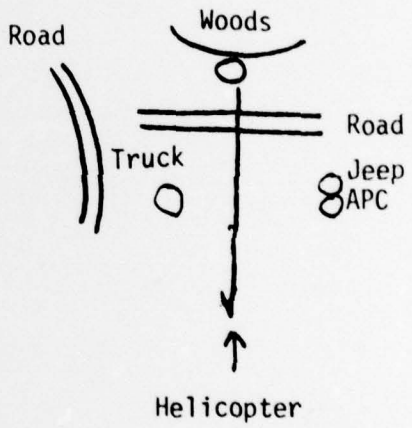

Tape Position 0328

A repeat of 0310 except that the moving APC is not as far past the other vehicles when the helicopter flies over. This means that some of the other targets are still in the frame the tracker is using for homing.

Tape Position 0349 - 0351

Rear aspect, close range images of five moving targets; 3 jeeps on the road and two APC's off the road.

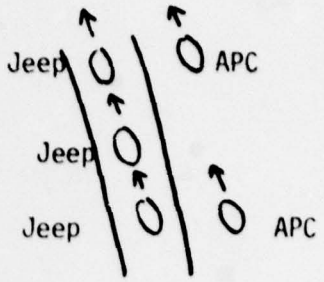

Tape Position 0356

Side view at close range of an APC, then a truck, and finally a closing sequence on the third APC.

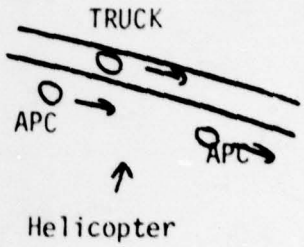

Tape Position 0364

The helicopter, at short range, is following behind the APC. The jeep and truck are shown in the background moving at high speed along the road. The second APC is then seen as is the last truck on the road.

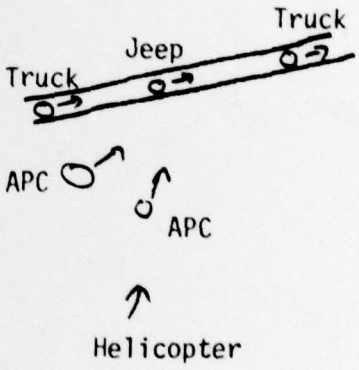

Tape Position 373

Acquisition at medium range of a truck and APC moving in parallel. The helicopter then closes on the APC with truck still in the image.

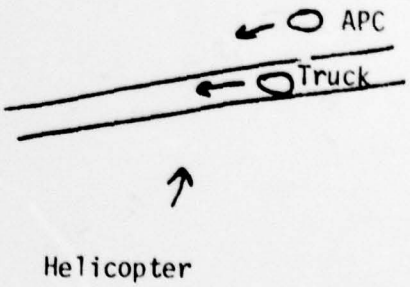

Tape Position 0381

Short range image of a moving APC as seen from the rear. The helicopter then swings onto the truck which is parked on the road and closes on the truck.

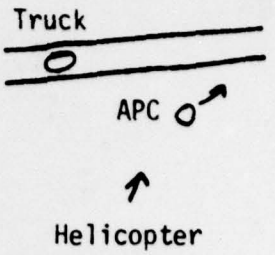

Tape Position 0387

Short range, closing sequence of an APC passing in front of a parked truck.

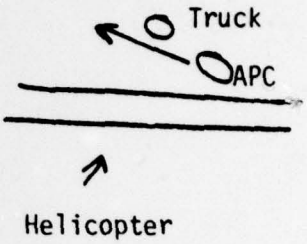

Tape Position 0394

Short range, rear aspect of a moving APC with the helicopter almost at ground level.

Tape Position 0400

Four targets are positioned along the edge of a clearing. Three are parked close together and their shapes merge. The targets are stationary. Acquisition is at medium to long range. The helicopter ends the run before it flies overhead.

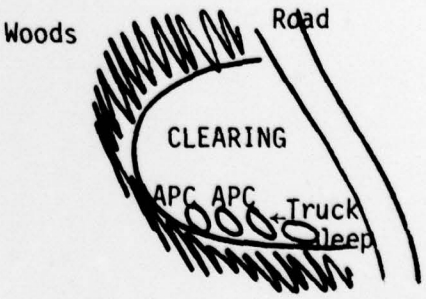

Tape Position 0420

A repeat of 0400 except at a greater helicopter altitude.

Tape Position 0436-0437

A view of the same targets at medium range and an even greater altitude.

Tape Position 0462-0469

A repeat of 0436 for longer duration.

Tape Position 0480-0489

Acquisition of the same target grouping at long range and the helicopter closes slowly to medium range as the run ends.

Tape Position 0493

Acquisition is obtained at long range and a different aspect angle by the helicopter. The helicopter then closes and loses altitude as it flies over simulating a munition.